



Université Mohamed Khider de Biskra
Sciences et de la Technologie
Département de Génie Mécanique

MÉMOIRE DE MASTER

Domaine : Sciences et Techniques

Filière : Génie Mécanique

Spécialité : Energétique

Réf. : Entrez la référence du document

Présenté et soutenu par :
Mounir Boukerche

Le : lundi 8 juillet 2019

Etudes expérimentales du séchage solaire par convection naturelle

Jury :

Dr.	Abdelmalek Boulegroun	MCB	Université de Biskra	Président
Dr.	Foued Chabane	MCA	Université de Biskra	Encadreur
Dr.	Rachid Athmani	PR	Université de Biskra	Examineur



Université Mohamed Khider de Biskra
Technological sciences
Department of mechanical engineering

MASTER Dissertation

Domain: Sciences and Techniques

Field: Mechanical Engineering

Specialty : Energetic

Réf. : Entrez la référence du document

Presented by :
Mounir Boukerche

Presented in: Monday 8 July 2019

Experimental studies of solar drying by natural convection

Jury :

Dr.	Abdelmalek Boulegroun	MCB	University of Biskra	President
Dr.	Foued Chabane	MCA	University of Biskra	Supervisor
Dr.	Rachid Athmani	PR	University of Biskra	Examiner

College year : 2018 - 2019

Dedications

I dedicate this work

To my dear parents

To my mother, may Allah have mercy on her

To my dear sisters

To my dear brothers

To my supervisor Dr. Chabane Foued

To all my colleagues and all my friends

*To all those who helped me and encouraged me during my
studies and for all those who are dear for me*

Boukerche Mounir

Thanking and appreciation

I thank Allah the Almighty who helped me to reach this advanced stage of the
academic level.

I would like to thank in the first place, my supervisor Dr. Chabane Foued on
his humility, his liberality, and his sacrifices to accomplish this work perfectly.

I would like to thank the members of jury, Dr. Boulegroun Abdelmalek as a
president and Dr. Athmani Rachid as an examiner for their accept to be
members of jury.

Also I would like to give a special thank to Mr. Guettala Ismail the responsible
of the technological hall, and all its workers, especially MR. Baaissi Lazher and
Mr. Sedrati Walid whose never hesitate to help.

Finally, I would like to thank my family, my friends and anyone who supported
me to finish this modest work.

«Nomenclature»

A_C : Aperture area of the absorber	(m ²)
d: product diameter	(mm)
D_{eff} : effective diffusivities	
e: product thickness	(mm, m)
G: solar radiation intensity	(W/m ²)
h: heat transfer coefficient	(W/m ² °C)
I_T : Total solar radiation incident on the collector	(W/m ²)
L : longitude	(°)
m: product mass	(kg)
\dot{m} : air mass flow rate	(Kg/s)
M_0 : initial moisture content	(%, wet basis)
M_d : Dry mass of product	(g) or (kg)
M_{eq} : equilibrium moisture content	(%, wet basis)
$M_{exp,i}$: the experimental moisture ratio	(%)
M_h : Humid mass of product	(kg)
$M_{mod,i}$: is the predicated moisture ratio	(%)
M_{out} : liquid mass loss	(g)
MR: moisture ratio	(%)
M_t : moisture content at any drying time	(%, wet basis)
N: the number of observations	
Q: Actual useful energy collected	(W)
R: correlation coefficient	
R^2 : factor de determination	
RH : relative humidity	(%)

RMSE: root mean square error

t: drying time (s,min,h)

T_a: ambient temperature (°C)

T_{ab}: average temperature of the absorbing plate (°C)

T_{ch}: drying chamber temperature (°C)

T_{in}: drying room inlet temperature (°C)

T_{product}: product temperature (°C)

V: air velocity (m/s)

x : Absolute humidity of a solid (kg/kg (*M_a*))

*X*²: chi square error

x_r : Moisture content on a humid basis (kg/kg (*M_h*))

η: solar collector efficiency (%)

φ : Latitude du lieu (°)

Figures list

Chapter I

Fig (I-1): Principle of solar heat collector.....	4
Fig (I-2): Functioning of plane solar collector.....	4
Fig (I-3): Exploded view of a flat-plate collector.....	6
Fig (I-4): A flat plat collector angle (winter-summer).....	6
Fig (I-5): Freeze dryer diagram.....	8
Fig (I-6): Principle of the osmotic dehydration.....	8
Fig (I-7): A desiccant wheel system for drying application.....	9
Fig (I-8): drying curves.....	12
Fig (I-9): Types of Solar Dryers.....	13
Fig (I-10): Direct Solar Dryers.....	14
Fig (I-11): The indirect solar dryer.....	15

Chapter II

Fig (II-1): Variation of moisture ratio with drying time for shade drying Δ , open sun drying, and solar dryer drying O.....	18
Fig (II-2): Variation of mass flow rate of the drying air with the solar irradiance (G_T).....	18
Fig (II-3): Hourly average temperature variations in the two solar dryers.....	19
Fig (II-4): Drying curves for Peppermint in the two dryers.....	19
Fig (II-5): Drying curves of two Peppermint species in dryer (b).....	19
Fig (II-6): Variation of experimental and predicted moisture content in tray 1 and 2 with drying time.....	20
Fig (II-7): Decreasing of moisture ratio of figs with drying time.....	20
Fig (II-8): Decreasing of moisture ratio of banana with drying time.....	20
Fig (II-9): Decreasing of moisture ratio of apple with drying time.....	21
Fig (II-10): Decreasing of moisture ratio of chili with drying time.....	21
Fig (II-11): Schematic view of experimental setup.....	21

Fig (II-12): Diurnal variation of the collector outlet air temperature, Temperature above each tray and atmospheric air temperature for the natural convection solar dryer for sample load conditions.....	22
Fig (II-13): Drying time vs moisture content.....	22
Fig (II-14): Drying time vs relative humidity.....	22
Fig (II-15): Picture of indirect forced circulation solar drying thermal system.....	23
Fig (II-16): Moisture ratio versus Time (h) curves.....	23
Fig (II-17): Wang and Singh model drying curve (Middle tray).....	23
Fig (II-18): Wang and Singh model (Middle tray) observed moisture content versus predicted moisture ratio for banana slice.....	23
Fig (II-19): Asparagus samples before drying (a) and after drying (b).....	24
Fig (II-20) : The variation of solar irradiation and mass of the product with respect to time for 78 and 48 no of asparagus samples ; MSR shows the mean solar irradiance in W/m ² for the 3 months, that is, Jun, July, and August ; Mass (Jun, July, and August) is the mass of the product of both 78 and 48 No. Samples of asparagus.....	24
Fig (II-21): schematic diagram of solar cabinet dryer.....	25
Fig (II-22): (a) moisture content vs time for solar cabinet dryer and (b) drying rate vs moisture Content for solar cabinet dryer.....	25
Fig (II-23): Photo of the tested solar dryer.....	26
Fig (II-24): The final dried product.....	26
Fig (II-25): Variation of moisture ratio versus drying time depicted at various airflow rates on different days.....	26
Fig (II-26): Comparison between experimental moisture ratios and that predicted for lemon blam calculated using the wang and singh model.....	26
Fig (II-27): Schematic of the drying system.....	27
Fig (II-28): Visual quality of the dried potato.....	27
Fig (II-29): variation of water content as function of time associated with one panel (a) and two panels (b).....	27
Fig (II-30): pictorial view of the solar drying system.....	28
Fig (II-31): Ginger samples (a) before drying; (b) after drying.....	28

Fig (II-32): Variations in moisture removing rate (% , dry basis) with respect to time (a) for 78 no, of ginger samples (b) for 48 no, of ginger samples.....	29
Fig (II-33): The laboratory scale of the solar swivel dryer.....	29
Fig (II-34): drying of tomato slices 3, 5 and 7 mm and fitted curves (a) (b) and (c) of the page model.....	30
Fig (II-35): Shape at the beginning and the end of drying.....	30
Fig (II-36): The experimental solar dryer.....	31
Fig (II-37): Products disposition for the first experimental set.....	31
Fig (II-38): Experimental with exponential approximation average dimensionless moisture ratio vs drying time for the four try of cube shape.....	31
Fig (II-39): Experimental with exponential approximation average dimensionless moisture ratio vs drying time for the four try of disc shape.....	31
Fig (II-40): Experimental with exponential approximation average dimensionless moisture ratio vs drying time for the four try of parallepepedic shape.....	31
Fig (II-41): Schematic diagram of the mixed-mode solar dryer. (The dimensions are in cm.).....	32
Fig (II-42): Variation of convective heat transfer coefficient with drying time for potato cylinders and slices.....	32
Fig (II-43): Variation of specific energy consumption with drying time for potato cylinders and slices.....	32
Fig (II-44): Photograph of the direct solar dryer.....	33
Fig (II-45): Variation in the mint moisture ratio with drying time.....	33
Fig (II-46): Variation in the mint-drying rate with drying time.....	34

Chapter III

Fig (III-1): Satellite picture of the experience area.....	37
Fig (III-2): Temperature and relative humidity curves of Biskra.....	38
Fig (III-3): Experimental setup (solar collector with drying chamber).....	38
Fig (III-4): Experimental setup of drying chamber.....	39
Fig (III-5): Orifices into drying chamber.....	39
Fig (III-6): Support of the drying product.....	40

Fig (III-7): Schematic view of balance system.....	40
Fig (III-8): The balance system modifications.....	41
Fig (III-9): A digital electronic balance machine.....	41
Fig (III-10): A thermometer-control (Model TPM-10).....	42
Fig (III-11): A thermocouples type k.....	42
Fig (III-12): Hygrometer (Model PCE-555).....	42
Fig (III-13): pyranometer (Model Voltcraft PL-110SM).....	43
Fig (III-14): A digital anemometer (Model KIMO-LVA).....	43
Fig (III-12): Wet and dried slices of potato with 1mm of thickness and 44 mm of diameter.....	44
Fig (III-13): Wet and dried slices of carrot with 1mm of thickness and 30mm of diameter.....	44
Fig (III-14): Wet and dried slices of apple with 1mm of thickness and 32mm of radius.....	44
Fig (III-15): Example of linear fitting.....	47
Fig (III-16): Calculation of a, b, R ² by using Microsoft Excel.....	50
Fig (III-17): Calculation of a, b, R ² by using Matlab program.....	51

Chapter IV

Fig (IV-2a): Variation of solar radiation intensity in 1-3 days of potato drying.....	56
Fig (IV-2b): Variation of solar radiation intensity in 1-3 days of carrot drying.....	57
Fig (IV-2c): Variation of solar radiation intensity in 1-3 days of apple drying.....	57
Fig (IV-3a): Average absorbing surface temperature versus time for three days of potato drying.....	58
Fig (IV-3b): Average absorbing surface temperature versus time for three days of carrot drying.....	58
Fig (IV-3c): Average absorbing surface temperature versus time for three days of apple drying.....	59
Fig (IV-4a): Variation of the drying room inlet temperature with time for 3 days of potato drying.....	60
Fig (IV-4b): Variation of the drying room inlet temperature with time for 3 days of carrot drying.....	60
Fig (IV-4c): Variation of the drying room inlet temperature with time for 3 days of apple drying.....	61

Fig (IV-5a): Variation of drying room temperature versus time for potato slices.....	62
Fig (IV-5b): Variation of drying room temperature versus time for carrot slices.....	62
Fig (IV-5c): Variation of drying room temperature versus time for apple slices.....	62
Fig (IV-6a): Variation of product temperature versus time for different thicknesses of potato slices.....	63
Fig (IV-6b): Variation of product temperature versus time for different thicknesses of carrot slices.....	64
Fig (IV-6c): Variation of product temperature versus time for different thicknesses of apple slices.....	64
Fig (IV-7a): The change in relative humidity of product versus time for potato drying.....	65
Fig (IV-7b): The change in relative humidity of product versus time for carrot drying.....	65
Fig (IV-7c): The change in relative humidity of product versus time for apple drying.....	66
Fig (IV-8a): Variation in liquid mass loss during time for potato drying.....	67
Fig (IV-8): Variation in liquid mass loss during time for carrot drying.....	67
Fig (IV-8c): Variation in liquid mass loss during time for apple drying.....	67
Fig (IV-9a): The moisture ratio versus drying time for different models of potato slices with 1, 1.5, and 2 mm of thickness.....	68
Fig (IV-9b): The moisture ratio versus drying time for different models of carrot slices with 1, 2 and 3mm of thickness.....	69
Fig (IV-9c): The moisture ratio versus drying time for different models of apple slices with 1, 2 and 3mm of thickness.....	70

Tables list

Chapter III

Table (III-1): Mathematical model applied to the drying curves.....	45
Table (III-2): Thin layer drying models for describing drying of potato slices.....	53
Table (III-3): Thin layer drying models for describing drying of carrot slices.....	53
Table (III-4): Thin layer drying models for describing drying of apple slices.....	53

Summary

Dedications.....	
Thanking and appreciation.....	
Nomenclature.....	
Figures list.....	
Tables list.....	
Summary.....	
General introduction.....	1

Chapter I: Application and process of solar drying

I.1. Introduction:.....	3
I.2. Solar collectors:.....	3
I.2.1. Technology of plane solar collectors:.....	3
I.2.1.1. Components of thermal converting system:.....	3
I.2.1.2. Principle of a plane solar collector:.....	3
I.2.1.3. Functioning of a plane solar collector:.....	4
I.2.1.4. The efficiency of solar collectors:.....	5
I.2.1.5. Components of solar air collectors:.....	5
I.2.1.6. Position and orientation of a collector:.....	6
I.2.2. Application for solar air collectors:.....	6
I.3. Generality on the drying:.....	7
I.3.1. Methods of drying:.....	7
I.3.1.1. Low-temperature drying:.....	7
I.3.1.2. High-temperature drying:.....	7
I.3.1.3. Freeze-drying:.....	7
I.3.1.4. Osmovac drying (Osmotic dehydration):.....	8

I.3.1.5. Desiccant drying:.....	9
I.3.2. Objectives of drying:.....	9
I.3.3. applications of solar drying:.....	9
I.3.3.1. Industrial solar drying:.....	9
I.3.3.2. Agricultural solar drying:.....	9
I.3.4. Terminology of drying:.....	10
I.3.4.1. Humidity:.....	10
I.3.4.2. Humidity rate:.....	10
I.3.4.3. Absolute humidity of a solid:.....	10
I.3.4.4. Relative humidity:.....	10
I.3.5. Effect of Parameters on drying:.....	11
I.3.5.1. Temperature:.....	11
I.3.5.2. Mass flow rate:.....	11
I.3.5.3. Relative humidity of air:.....	11
I.3.5.4. Moisture Content of the drying Product:.....	12
I.3.6. Drying speed:.....	12
I.3.7. Drying rate periods:.....	12
I.4. Classification of solar dryers:.....	13
I.4.1. Active dryers:.....	13
I.4.2. Passive dryers:.....	13
I.4.3. Integral Type Dryer (direct):.....	14
I.4.3.1. Advantages and disadvantages:.....	14
I.4.4. Distributed dryers (indirect):.....	14
I.4.4.1. Advantages and disadvantages:.....	15
I.5. Conclusion:.....	15
References:.....	16

Chapter II: Bibliographic study

II.1. Introduction:.....	18
II.2. Bibliographic study:.....	18
II.3. Conclusion :.....	34
References:.....	35

Chapter III: Experimental and theoretical study

III.1. Introduction:.....	37
III.2. Experiments location and zone climate:.....	37
III.2.1. Experiments location:.....	37
III.2.2. Experiments zone climate:.....	38
III.3. Experimental study:.....	38
III.3.1. Manufacture of the drying chamber:.....	39
III.3.2. The balance system modification:.....	40
III.3.3. Experimental Procedure:.....	41
III.4. Theoretical study:.....	44
III.4.1. Calculation of effective diffusivities:.....	46
III.4.2. Thin layer drying model:.....	46
III.4.3. Least Squares method:.....	47
III.4.4. Linearization of Nonlinear Behavior:.....	47
III.4.5. Determination of the model constants:.....	48
III.4.6. Application of the least square method:.....	49
III.4.6.1. Example of Microsoft Excel:.....	49
III.4.6.2. Example of Matlab:.....	51
III.5. Conclusion:.....	54
References:.....	55

Chapter IV: Results and discussion

IV.1. Introduction:.....	56
IV.2. Variation in solar radiation intensity:.....	56
IV.3. Variation of the average temperature of the absorber plate:.....	58
IV.4. variation of drying room inlet temperature:.....	59
IV.5. Variation of drying room temperature:.....	61
IV.6. Variation of product temperature:.....	63
IV.7. The change in relative humidity of products:.....	64
IV.8. The change in liquid mass loss during time of each product:.....	66
IV.9. Determination of reduced moisture ratio MR:.....	68
IV.10. Conclusion:.....	71
General conclusion.....	
Abstract.....	

«General introduction»

The sun has enabled life on our planet, and our life cannot be imagined without it.

This was recognized and celebrated by all the cultures already in the ancient ages, the use of the very clean solar energy is not a new discovery of the scientist of our days. It was used in diverse scopes since a lot of centuries, and that confirms the history of solar energy conversion is long, various and exciting.

The energy received on earth from the sun is known as the solar energy, which is defined as the energy emitted from the sun mainly in the form of heat and light, and it is the product of nuclear interactions inside the star closest to us and it is the sun. It is considered as a primary resource of energy that guarantees life continuation on earth. This energy is very important in the earth and the organisms on its surface. It is one of most renewable energies uses because of its daily availability, and the most essential that it is free and inexhaustible. The principal use of this energy based on capturing the sun light and subsequently converting it into electricity or use it to air heating as needed.

The solar energy has many important applications including solar drying which is considered as a common technique between all the other applications, the solar drying is known as the process of humidity removing from a wet product like fruits and vegetables to conserve it and use it as needed in any time.

In the past, food was dried by exposing it directly to the sunrays due to the absence of appropriate technology for this process. But now there are many ways to accomplish the drying process like the indirect method, which is based on a solar air collector to increase the heating of air, and drying room to conserve the product to be dried from microbes in the outside and to isolate the emitted heat in a smaller space.

Solar drying varies from region to another, and to ensure the success of this process; the appointed region must have a high ambient temperature and a high solar radiation intensity, and the drying time and maintenance of the product quality are the basic criteria for selecting the appropriate drying method.

The Solar drying in Algeria is one of the processes that have found applications, because of the important quantities of solar irradiations that can be exploited in this country.

Nevertheless, the experience of Algeria in solar drying is recent and limited to drying of fruits, vegetables, medicinal and aromatic herbs.

The main purpose of this dissertation is to investigate the solar drying behaviour of thin layer drying for three different agricultural products potato, carrot and apple by using an indirect solar dryer and drying room under natural convection, in addition to determine a mathematical model by using the experimental data to calculate the moisture ratio of this drying behaviour.

Our dissertation consist of four chapters:

The first chapter presents a review of the importance of solar collectors and describes the process of solar drying and all the necessary to realize it.

The second chapter consist of the second chapter consist of a bibliographic study and presents a several previous studies that have a common purposes with our work.

The third chapter describes the experiment steps and show all measuring tools and the necessary materials to ensure the drying operation, also the method of the model determination.

The last chapter explains and interprets the obtained experimental results, which were translated into curves, and it gives comparisons between the used models.

Chapter I

Application

and

process of solar drying

I.1. Introduction:

Solar drying it is one of most old processes of agricultural products conservation used by humans. Solar drying is often differentiated from ‘sun drying’ by the use of equipment to collect the sun’s radiation to use it for drying of agricultural products.

So in this first chapter we are going to see the different methods and ways of solar drying, and present the functioning and the components of solar collectors that are more effective in the drying, also define the types of existing dryers and what are they used for.

I.2. Solar collectors:

Solar energy collector is a special type of heat exchanger that transforms solar radiation energy into internal energy of the transport medium. Basically, there are two types of flat-plate solar heating collectors; water heating collectors and air heating collectors. The pace of development of air heating collector is slow compared to water heating collector mainly due to lower thermal efficiency. Solar air collectors are widely used for low to moderate temperature applications like space heating, crop drying, and other industrial applications [1].

I.2.1. Technology of plane solar collectors:

I.2.1.1. Components of thermal converting system:

Any system for converting solar energy must be composed of the following necessary elements [2]:

- A surface for capturing of solar radiation.
- A heat transfer circuit, which ensure the transfer of extracted energy of collector to the accumulation element. Generally the heat transfer fluids used are water and air.
- A thermal storage.
- A distribution system.

I.2.1.2. Principle of a plane solar collector:

The principle of any solar collector at low temperature is bound by the greenhouse effect see figure (I-1). Is explained by the fact that the glass is a transparent material to solar radiation (at short wavelengths) While it is almost opaque to infrared radiation (at the long wavelengths).

The solar flux that runs through the glazing and going to heat the absorber is confined among them. Since the radiation emitted by this body mainly in the infrared can't through the glass [3].

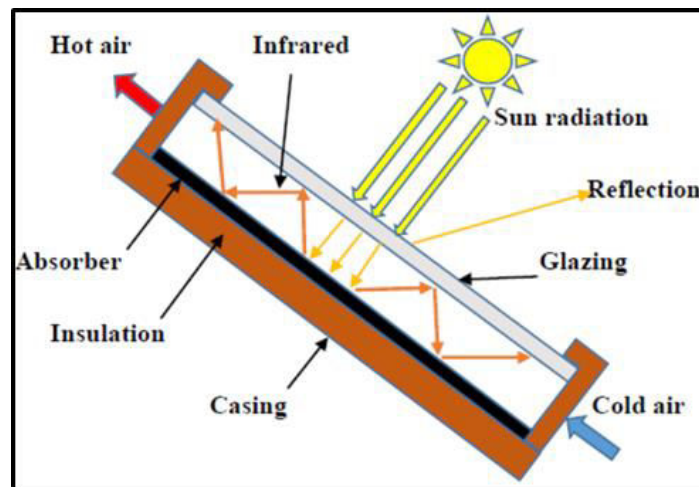


Fig (I-1): Principle of solar heat collector.

I.2.1.3. Functioning of a plane solar collector:

The functioning of a solar collector is started by the solar radiation, which goes through the glazing see figure (I-2), the body that is used to capture radiation called absorber, is usually dark in order to increase his absorption coefficient. The absorbing surface absorbs incident energy that it transmits by the exchange surface intermediary to a heat transfer fluid. The hot surfaces Exchange heat with the environment by radiation, conduction or convection [3].

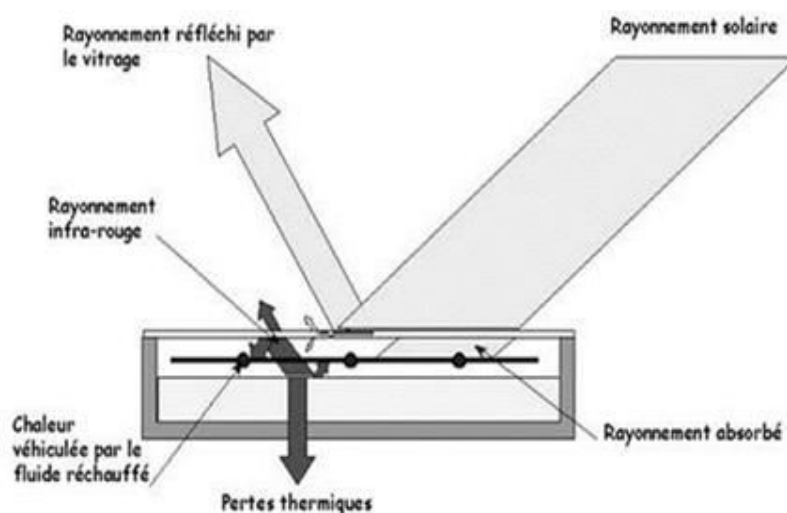


Fig (I-2): Functioning of plane solar collector [4].

I.2.1.4. The efficiency of solar collectors:

The efficiency of the solar collectors depends on the collector covered material; air velocity, the absorber and his place in the collector, the main efficiency parameter of a solar collector is the air heating degree [5], the instaneous solar collector efficiency η is defined as [6]:

$$\eta = \frac{\text{Actual useful energy collected}}{\text{Solar energy incident on the collector}} = \frac{Q}{I_T \cdot A_C} \quad (\text{I-1})$$

Where:

Q : Actual useful energy collected [W].

I_T : Total solar radiation incident on the collector [W/m²].

A_C : Aperture area of the absorber [m²].

I.2.1.5. Components of solar air collectors:

The solar collectors have been built in a wide variety of designs and from many different materials see figure (I-3), some of these principle materials are [7]:

- **Glazing:** One or more sheets of glass or other diathermanous (radiation-transmitting) material. This transparent cover is used to reduce convection losses. It also reduces radiation losses from the collector as the glass is transparent to the short wave radiation received by the sun but it is nearly opaque to long-wave thermal radiation emitted by the absorber plate (greenhouse effect).
- **Stream, fins, or passages:** To conduct or direct the heat transfer fluid from the inlet to the outlet.
- **Absorber plates:** To which the tubes, fins, or passages are attached. The plate may be integral with the tubes. Usually black colour is used, the absorber has a high thermal conductivity, its surface is coated to maximize radiant emission.
- **Headers or manifolds:** To admit and discharge the fluid.
- **Insulation:** To minimize the heat loss from the back and sides of the collector.
- **Container or casing:** To surround the aforementioned components and keep them free from dust, moisture, etc.

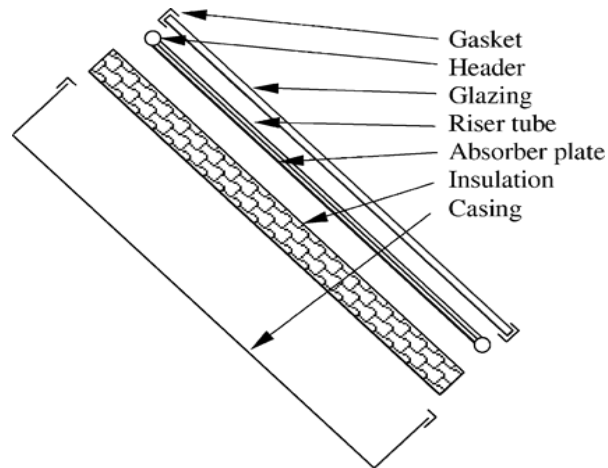


Fig (I-3): Exploded view of a flat-plate collector [7].

I.2.1.6. Position and orientation of a collector:

Sun's height on the sky is changing almost every week of the year. The highest is in summer when is the best time for collector and the lowest in winter see figure (I-4). Collectors are usually fixed in position and require no tracking of the sun. The collector should be oriented directly towards the equator, facing South in the northern hemisphere and North in the southern. The optimum tilt angle of the collector is equal to the latitude of the location with angle variations of **10** to **15°** more or less depending on the application [7].

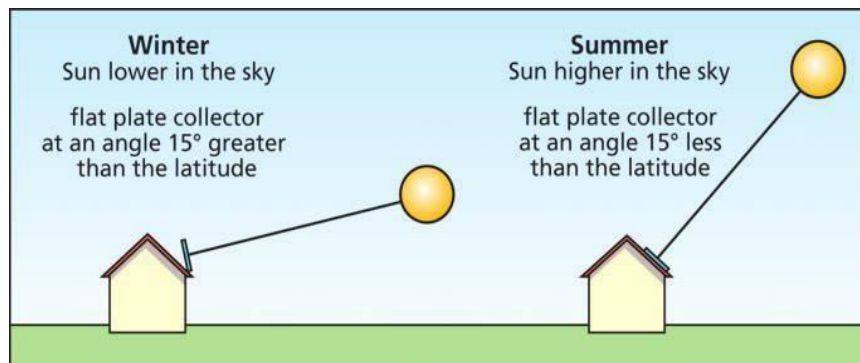


Figure (I-4): A flat plat collector angle (winter-summer).

I.2.2. Application for solar air collectors:

The solar air collector can be used for:

- **Industrial purposes:** Drying minerals, coal, bricks, food industry products, space heating for warehouses, factories, etc.

- **Agricultural purposes :** Drying grains, fruit, vegetables, meat, etc.
- **Household purposes:** Space heating small driers.
- **Community and commercial purposes:** Space heating for public buildings, office buildings, shopping centers.
- **Camping purposes:** Space heating for emergency relief camps or military camps.

I.3. Generality on the drying:

Drying is defined as a process of moisture removal due to simultaneous heat and mass transfer. It is a classical method of food preservation, which provides longer shelf-lifetime weight for transportation and small space for storage. The drying process takes place in two stages:

- The first stage happens at the surface of the drying material at constant drying rate and is similar to the vaporization of water into the ambient.
- The second stage takes place with decreasing (falling) drying rate. The condition of the second stage determined by the properties of the material being dried [8].

I.3.1. Methods of drying:

There are many methods and ways that can be used in the drying as:

I.3.1.1. Low-temperature drying:

It is used for places where the average ambient temperature is around 10 °C. The temperature range used for this type of drying ranges from 15 to 50 °C. It uses natural or heated air with low temperature to dry the product in very longer time. Even though it is a relatively slower process and is dependent on favourable weather conditions [9].

I.3.1.2. High-temperature drying:

High-temperature drying uses temperature starting from 50 °C and this is the most common method in developed countries. It is used for drying high moisture content products such as fruits and vegetables. A hot air recirculation system may be employed with a dehumidification unit for increase the effectiveness of the system with less wastage of the energy [9].

I.3.1.3. Freeze-drying:

Freeze-drying is a drying process in which the solvent or the suspension medium is crystallized at low temperature, thereafter sublimed from the solid state directly into the vapor phase. The goal of freeze-drying is to produce a substance with good shelf stability and which is unchanged after reconstitution with water, although this depends also very much on last step of the process; the packing and condition of storage [10].

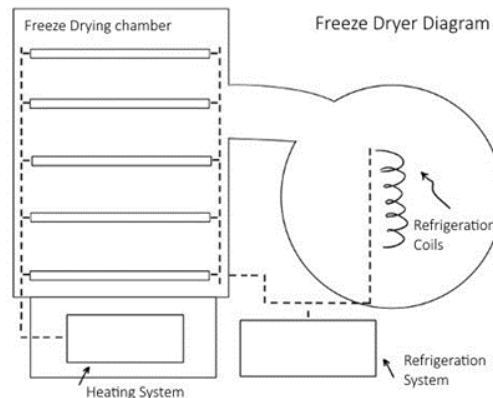


Fig (I-5): Freeze dryer diagram.

I.3.1.4. Osmovac drying (Osmotic dehydration):

Osmotic dehydration (OD) is a water removal technique, which is applied to horticultural products such as fruits and vegetables to reduce the water content. The osmotic dehydration is a useful technique for the production of safe, stable, nutritious, tasty, economical, and concentrated food obtained by placing the solid food, whole or in sliced in sugar or salt aqueous solutions of high osmotic pressure [11].

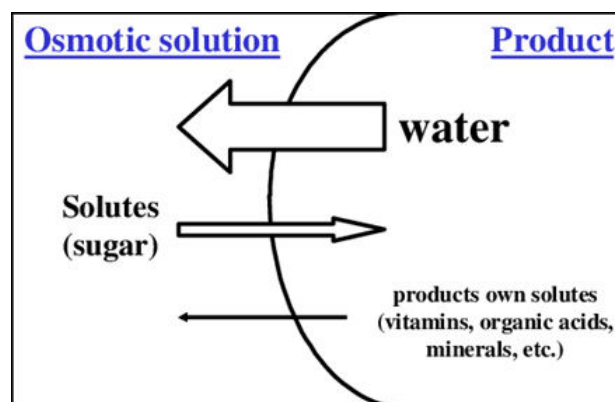


Fig (I-6): Principle of the osmotic dehydration.

I.3.1.5. Desiccant drying:

It is one of the best methods for dehydrating the exhaust air for recirculation, if the exhaust air is still hot. Hence, the efficiency of the system can be improved. The desiccant can be regenerated using solar heat [9].

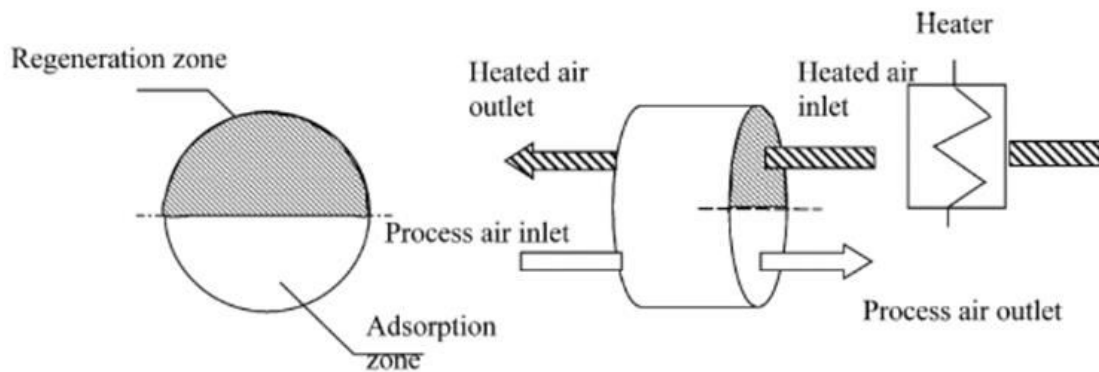


Fig (I-7): A desiccant wheel system for drying application [12].

I.3.2. Objectives of drying:

The major objectives of the drying process are as follows [9]:

- To reduce the food spoilage caused by larger production and limited usage.
- Prolonged usage of the product preventing them from spoiling due to microbial attacks.
- Drying will reduce the weight dramatically and makes transportation easy.
- High-quality dried product will have good market value and hence will bring high profit to the producers.

I.3.3. applications of solar drying:

The numerous solar drying applications are classified into two main categories, that is, agricultural and industrial [13].

I.3.3.1. Industrial solar drying:

The application of solar drying in industrial sectors can be investigated for different materials, such as biomass, brick, textile, cement, polymers, paper and allied products,

and timber as well as for different processes, such as drying of porous materials, wastewater treatment, and pharmaceutical processes. For instance, the use of solar dryers in wastewater treatment reduces expenses and the duration of the conventional drying process.

I.3.3.2. Agricultural solar drying:

Is an essential process in the preservation of agricultural crops such as s paddy, oil seed, carrot, herb and spices, and vegetables.

I.3.4. Terminology of drying:

I.3.4.1. Humidity:

This term indicates the liquid contained in the solid or liquid body, and which will have to eliminated due to drying.

I.3.4.2. Humidity rate:

It is the liquid mass contained per unit mass of material to be dried, or it is the rate between the mass of the liquid contained in the humid body on the mass of the body.

I.3.4.3. Absolute humidity of a solid:

Also known as moisture content on a dry basis, it is simply the mass of the liquid contained in the product compared to its dry mass.

$$x = \frac{M_h - M_d}{M_d} \quad (\text{I-2})$$

Where:

x : Absolute humidity of a solid [**kg/kg** (M_d)]

M_h : Humid mass of product [**kg**].

M_d : Dry mass of product [**kg**].

I.3.4.4. Relative humidity:

Also known as moisture content on a humid basis, it is the mass of the liquid contained in the product compared to its humid mass.

$$x_r = \frac{M_h - M_d}{M_h} \quad (\text{I-3})$$

Where:

x_r : Moisture content on a humid basis [kg/kg (M_h)].

M_h : Humid mass of product [kg].

M_d : Dry mass of product [kg].

I.3.5. Effect of Parameters on drying:

The most important parameters, which determine the quality of the dried product, are mentioned below [9]:

I.3.5.1. Temperature:

Drying temperature is a major deciding factor, which mainly determines the quality of the dried product. High drying temperature may impair the germination capacity of seeds and can damage the product changing either the chemical combination or smoulder the product. Lower drying temperature may lead to longer drying time which may lead microbial contamination.

I.3.5.2. Mass flow rate:

Mass flow rate also plays an important role in drying process. Optimum mass flow rate is designed using the temperature requirement and the maximum air velocity, which can be maintained, inside the drying chamber.

I.3.5.3. Relative humidity of air:

The relative humidity of air is an important factor same as that of temperature because humidity gradient between air and the product will be a major driving force in a natural convection system. Lower relative humidity of the air can increase the drying rate and will help in reducing the drying time.

I.3.5.4. Moisture Content of the drying Product:

The moisture content of the product to be dried is an important factor for determining the quality of the product and thereby the market value. Products with higher moisture content are found to have lesser drying time than those having very lesser moisture content.

I.3.6. Drying speed:

This drying rate for a product is the variation of its average water content as a function of time.

It represents the evaporation power related to the properties of the product under the conditions of the process [14]:

$$\dot{X} = \frac{dX}{dt} = -k(X_f - X_0) \quad (\text{I-4})$$

Where: k is the time constant (s^{-1}).

I.3.7. Drying rate periods:

For each product, there is a representative curves that describes the drying characteristics for that product at specific temperature, velocity and pressure conditions. The fig (I-8) shows a typical drying curve. The variations in that curve will occur principally in relative rate to carrier velocity and temperature [15].

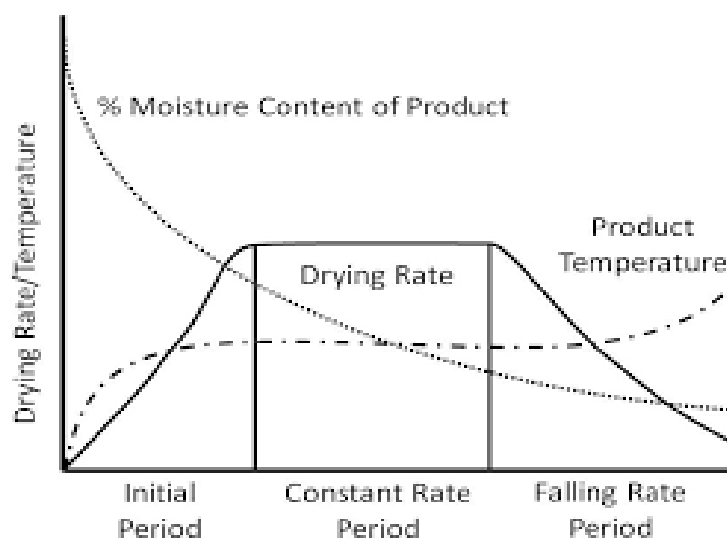


Fig (I-8): drying curves [15].

- **The first phase:** initial rate period or increasing rate period.
- **The second phase:** constant rate period.
- **The third phase:** falling rate period.

I.4. Classification of solar dryers:

Solar dryers are available in different types and different ranges for various applications, and they can be classified into two major groups, as [16]:

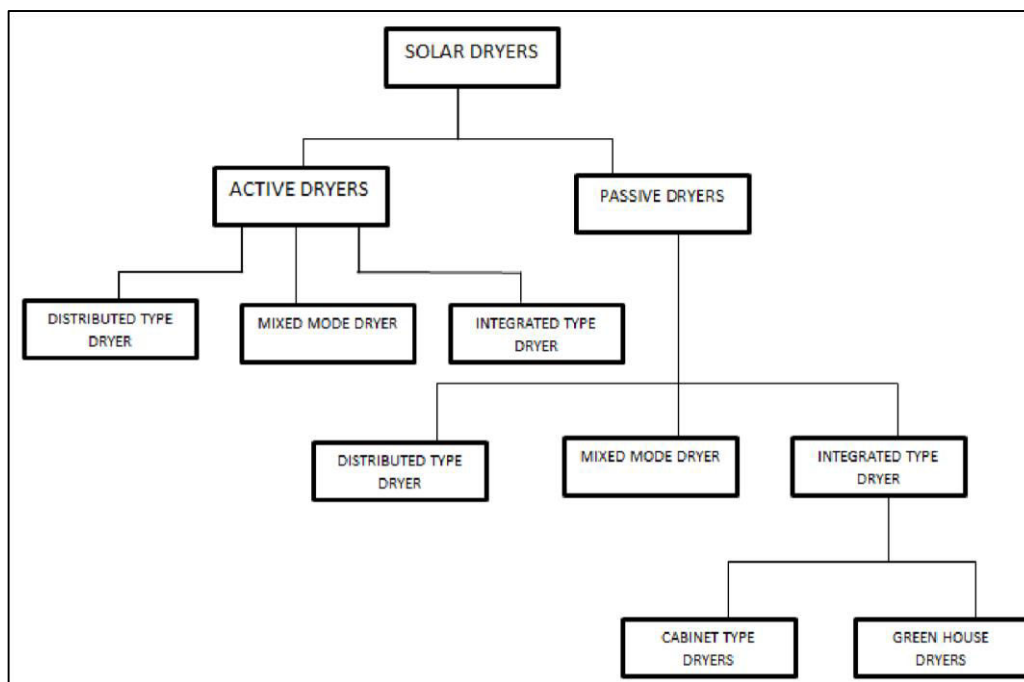


Fig (I-9): Types of Solar Dryers [16].

I.4.1. Active dryers:

Active solar drying systems are designed incorporating external means, like fans or pumps, for moving the solar energy in the form of heated air from the collector area to the drying beds. Thus all active solar dryers are, by their application, forced convection dryer.

I.4.2. Passive dryers:

In a passive solar dryer, air is heated and circulated naturally by buoyancy force or as a result of wind pressure or in combination of both. Normal and reverse absorber cabinet dryer and greenhouse dryer operates in passive mode. Passive drying of crops is still in common practice in many Mediterranean, tropical and subtropical regions especially in Africa and Asia or in small agricultural communities.

There are two principal distinct sub-classes of either the active passive solar dryers can be identified as:

I.4.3. Integral Type Dryer (direct):

In Integral type dryers the moisture is removed from top; air enters into cabinet from below and leaves from top, and the food product is covered with the glass cover. When sun light fall on the surface of glass then three things happens, first is some light is absorbed, some light is reflected back from the glass, and some light is transmitted, see figure (I-10).



Fig (I-10): Direct Solar Dryers [17].

I.4.3.1. Advantages and disadvantages [18] :

- Contamination of product due to enclosure with transparent cover is less.
- Product quality obtained is higher than open to the sun drying.
- Time required for product drying is same as sun or natural drying.

I.4.4. Distributed dryers (indirect):

This type of dryer differs from direct dryer by heat transfer and vapor removal. In this method, atmospheric air heated in flat plate collector then this hot air from flat plate collector is flow in the cabin where products are placed. The moisture from this type of dryer is removed by convection as well as by diffusion, see figure (I-11).



Fig (I-11): The indirect solar dryer [19].

I.4.4.1. Advantages and disadvantages [18] :

- This technique avoids contamination of final product.
- It is very efficient method than the direct type of solar drying.
- Maintain the quality of product by avoiding direct exposure in solar radiations.
- Time required for drying some product is less.
- Requires more initial cost.
- Need maintenance after particular period.

I.5. Conclusion:

This first chapter has allowed us to take look on the solar drying that it is one of most renewable energies applications, it depends on a several ways or multiple techniques and tools to achieve it in good conditions. Basically, the solar drying is based on a special methods and materials as needed for achieving its necessary objectives and to ensure the drying process in the best way.

«References»

[1]: Ramani, B. M., Akhilesh Gupta, and Ravi Kumar. "Performance of a double pass solar air collector." *Solar Energy* 84.11 (2010) : 1929-1937.

[2] : Fares, A., Etude et optimisation du séchage solaire indirect des produits agro-alimentaires dans la région de Biskra, thème de master, Biskra, université Mohamed Kheider, 2018, p5.

[3] : Daouda Tine, M., dimensionnement d'un capteur solaire plan par la méthode nodale, projet de fin d'études, Dakar, université cheikh Anta Diop de Dakar, 2002.

[4] : Etude de faisabilité d'un climatiseur solaire adapté à la région de Biskra – Scientific Figure on ResearchGate. Available from: https://www.researchgate.net/Principe-de-fonctionnement-dun-capteur-solaire-thermique-plan-Andre-and-Thomas-2008_fig6_323556891 [accessed 3 Nov 2018].

[5]: Aboltins, Aivars, et al. "Investigations of air solar collector efficiency." *Proceedings of the 8th International Scientific Conference on Engineering for Rural Development Engineering for Rural Development*. Vol. 1. 2009.

[6]: Garg, H. P., J. prakash (2000, 1997) *Solar Energy Fundamentals and Applications: First Revised Edition*, New Delhi, and Tata McGraw-Hill.

[7]: KALOGIROU, soteris A. Solar thermal collectros and applications. *Progress in energy and combustion science*, 30(3), 231-295.

[8]: El-Sebaili, A. A., and S. M. Shalaby. "Solar drying of agricultural products: A review." *Renewable and Sustainable Energy Reviews* 16.1 (2012): 37-43.

[9]: Aravindh, M. A., and A. Sreekumar. "Solar drying—a sustainable way of food processing." *Energy sustainability through green energy*. Springer, New Delhi, 2015. 27-46.

[10]: Oetjen, Georg-Wilhelm, and Peter Haseley. *Freeze-drying*. John Wiley & Sons, 2004.

[11]: Chandra, Suresh, and Durvesh Kumari. "Recent development in osmotic dehydration of fruit and vegetables: a review." *Critical Reviews in Food Science and Nutrition* 55.4 (2015): 552-561.

[12]: Chua, K. J., and S. K. Chou. "Low-cost drying methods for developing countries." *Trends in Food Science & Technology* 14.12 (2003): 519-528.

[13]: Pirasteh, G., et al. "A review on development of solar drying applications." *Renewable and Sustainable Energy Reviews* 31 (2014) : 133-148.

[14] : A. Labeled, Contribution à l'étude des échanges convectifs en régime transitoire dans les Capteurs Solaires Plans à air ; Application au séchage des produits agro-alimentaires. Thèse de Doctorat. Université Mohamed Khider-Biskra (2012).

[15] : Rahmanta MA, Felani MI. Application of Rotary Drum Dryer at Ombilin Coal Fired Power Plant. *International Journal of Materials, Mechanics and Manufacturing*, Vol. 3, No. 3, August 2015.

[16]: Balasuadhakar, A., et al. "A Review on Passive Solar Dryers for Agricultural Products." *Int. J. for Innovative Research in Science & Technology* 3 (2016): 64-70.

[17]: Ameri, Billal, et al. "Comparative approach to the performance of direct and indirect solar drying of sludge from sewage plants, experimental and theoretical evaluation." *Solar Energy* 159 (2018) : 722-732.

[18]: Sontakke, Megha S., and Sanjay P. Salve. "Solar drying technologies: A review." *International Journal of Engineering Science* 4 (2015): 29-35.

[19]: Boulemtafes-Boukadoum, Amel, and Ahmed Benzaoui. "Energy and exergy analysis of solar drying process of Mint." *Energy Procedia* 6 (2011): 583-591.

Chapter II

Bibliographic Study

II.1. Introduction:

The solar drying is a very wide field, and its applications varies in many ways and different techniques as needed by using a special materials, for this reason a lot of studies have been carried out on solar drying, so we are going to see in this second chapter a several of articles and dissertations which contains some of previous experimental studies about the solar drying of agricultural products and their different techniques and the exploited equipments on this operation.

II.2. Bibliographic study:

D.R. Pangavhane et al [1]:

In this study, grapes were successfully dried in the developed natural convection solar dryer, which consist of a solar air heater and a drying chamber. This system can be used for drying various agricultural products like fruits and vegetables. The qualitative analysis showed that the traditional drying, shade drying and open sun drying, dried the grapes in 15 and 7 days respectively, while the solar dryer took only 4 days and produced better quality raisins.

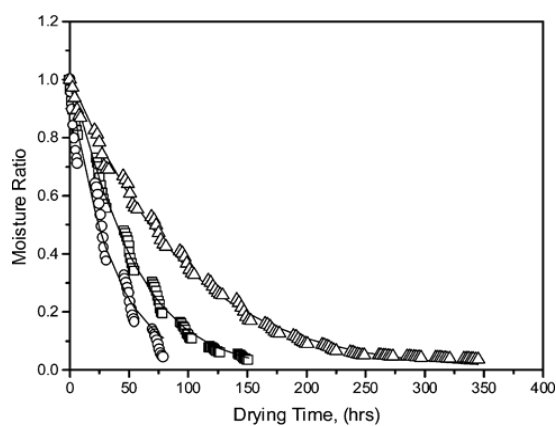


Fig (II-1): Variation of moisture ratio with drying time for shade drying Δ , open sun drying, and solar dryer drying O.

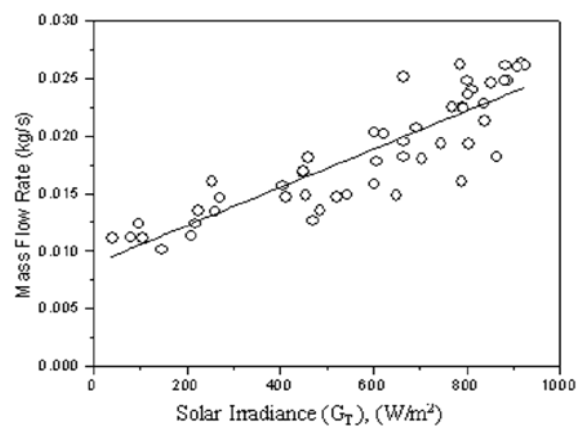


Fig (II-2): Variation of mass flow rate of the drying air with the solar irradiance (G_T).

H. S. Abdel-Galil et al [2] :

The main objective of this research work was to investigate the effect of a direct (a) and indirect (b) natural convection solar drying systems on quality of two species of peppermint namely: *mentha pepperita* and *mentha vridis*.

The obtained results indicated that the air temperature in the dryers increased above ambient (36.4°C) by maximum values of 14.2°C and 9.6°C for dryers (a) and (b), respectively. The daily average thermal efficiencies for dryers (a) and (b) were 36.60% and 35.70%, respectively.

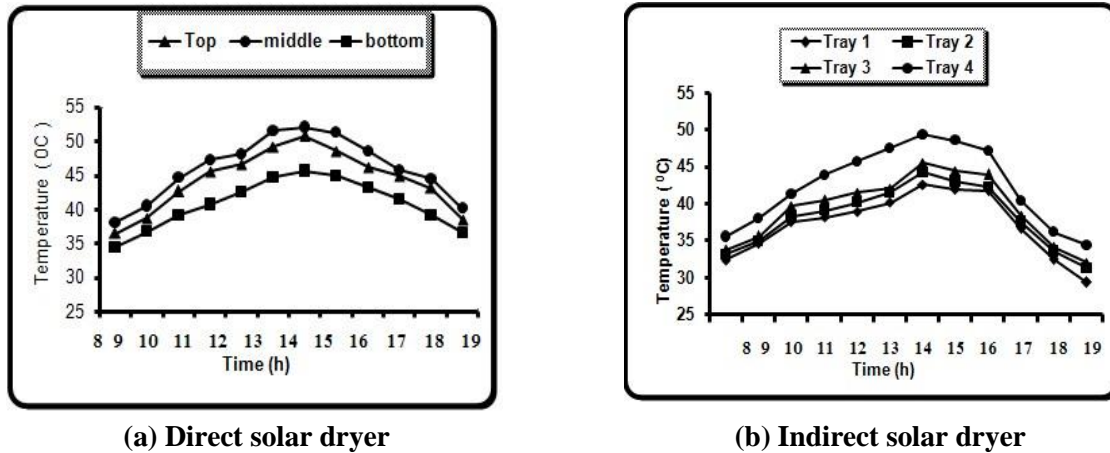


Fig (II-3): Hourly average temperature variations in the two solar dryers.

Dryer (a) achieved the fast rate of peppermint moisture content reduction as compared with dryer (b). On the basis of the effective collector areas, the estimated moisture removal rates were 3.57 and $3.53 \text{ kg} \cdot \text{m}^{-2} \cdot \text{day}^{-1}$ for dryers (a) and (b), respectively. The water loss from *mentha pepperita* (72.4% w.b.) was higher than that lost from *mentha vridis* (65.2% w.b.).

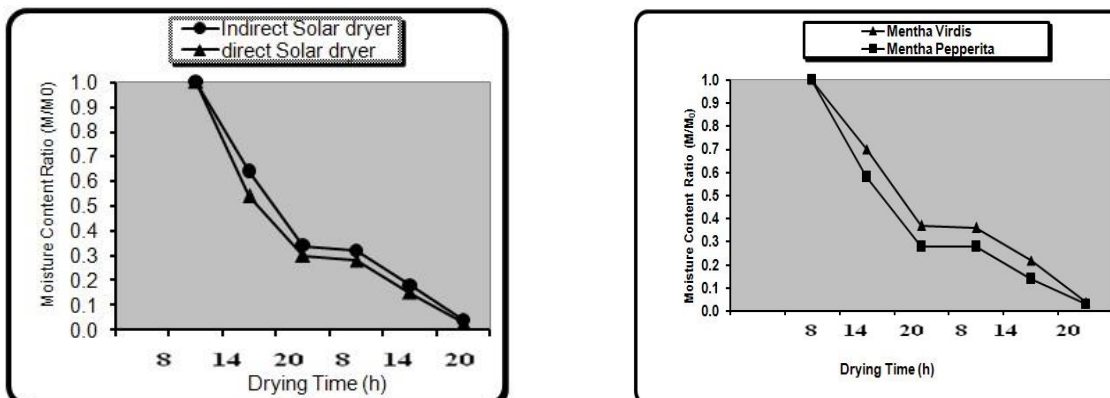


Fig (II-4): Drying curves for Peppermint in the two dryers.

Fig (II-5): Drying curves of two Peppermint species in dryer (b).

M. Ayadi et al [3]:

The objective of this experimental work, was to investigate the energy and economic performance of a totally solar drying unit with storage for aromatic and medicinal plants, to dry a quantity of a given agricultural products during 1 day of harvest season.

Drying experiments were conducted for spearmint grown in Tunisia. It was observed that this unit is able to dry more than 2.5 kg of spearmint per day with a moisture reduction efficiency of 70%. It was found that for all the period of harvest, so for 5 months assumed dryer used per year, the payback period is 3.6 years.

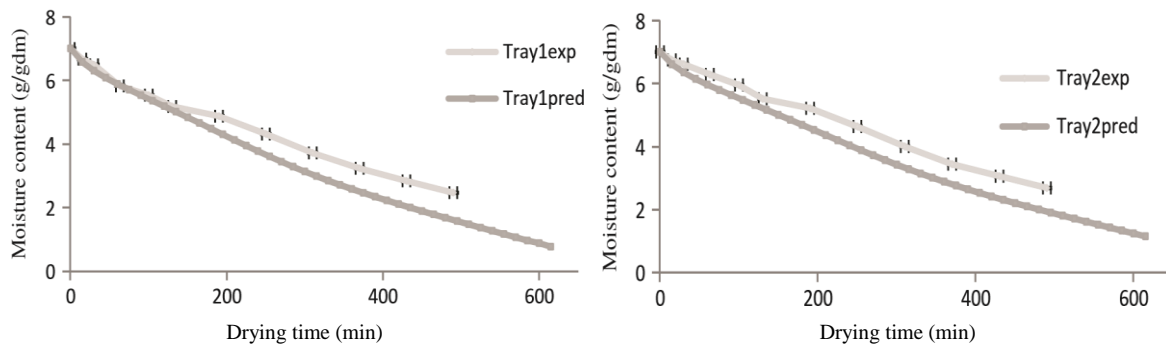


Fig (II-6): Variation of experimental and predicted moisture content in tray 1 and 2 with drying time.

AL- Khuresi N et al [4] :

This research is a try to develop a solar dryer for figs. The aim is to produce a drying fig with good quality and decrease the drying time. Five different indirect design concepts were presented. All concepts that generated are indirect forced and natural convection of solar energy. One design concept was chosen after screening process, which consists of a solar collector, a drying chamber, and chimney. Finally, the result was discussing five experiments that did to obtain the higher performance of solar dryer. The result recorded the average chamber temperature is 59°C compared with average ambient temperature is 32 °C. The theoretically result presented the dryer efficiency is 17.6%.

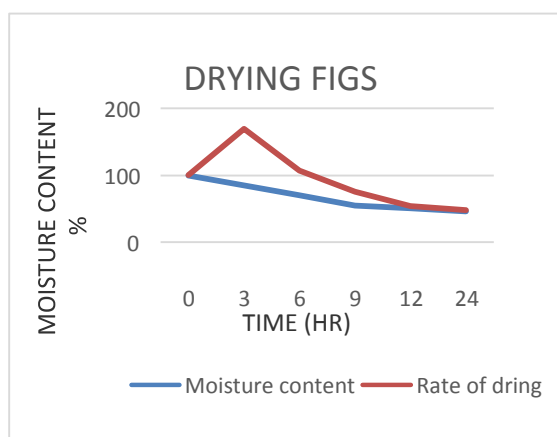


Fig (II-7): Decreasing of moisture ratio of figs with drying time.

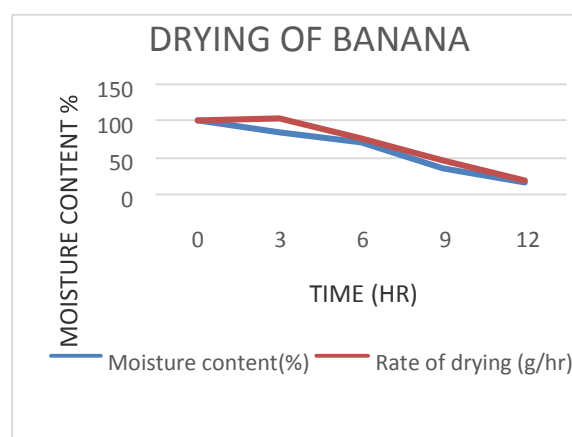


Fig (II-8): Decreasing of moisture ratio of banana with drying time.

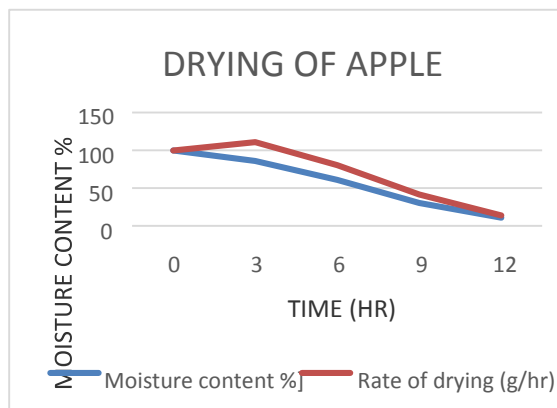


Fig (II-9): Decreasing of moisture ratio of apple with drying time.

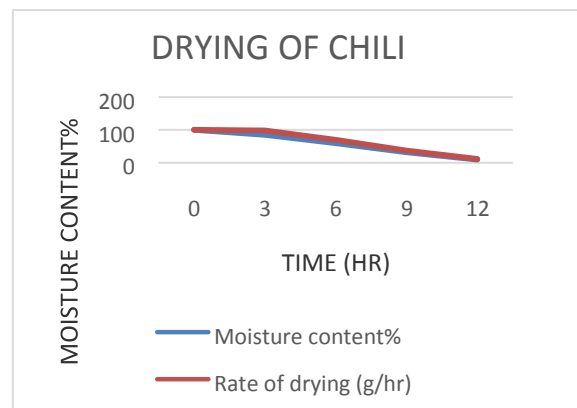


Fig (II-10): Decreasing of moisture ratio of chili with drying time.

Abhay Lingayat et all [5]:

The aim of their experiment was to study drying characteristics of banana by using an indirect type solar dryer, was designed and developed to dry agricultural products. The qualitative analysis for drying of banana showed that moisture content of banana was reduced from initial value of 356% (db) to final moisture content of 16.3292%, 19.4736%, 21.1592%, 31.1582%, and 42.3748% (db) for Tray1, Tray2, Tray3, and Tray4. And open sun drying respectively and they observed that the temperature of drying air is the most important and effective factor during drying. The humidity of air as well as air velocity is also an important factor for improving the drying rate.

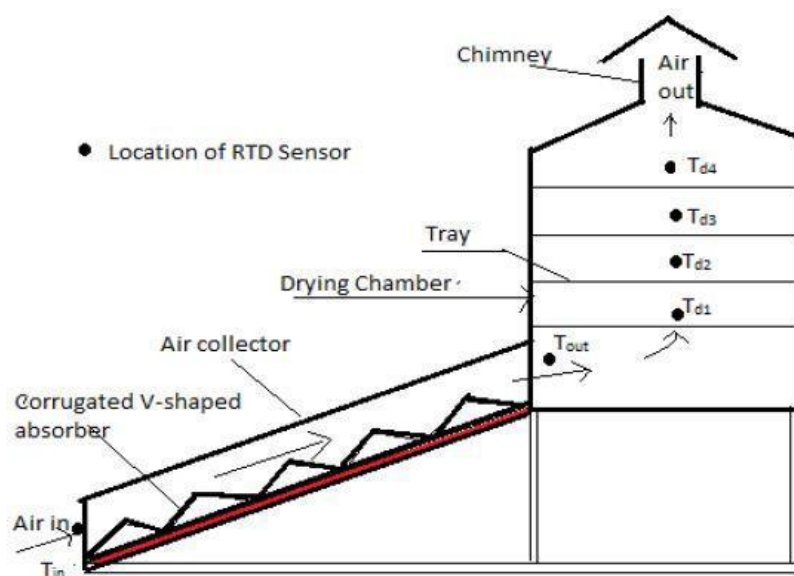


Fig (II-11): Schematic view of experimental setup.

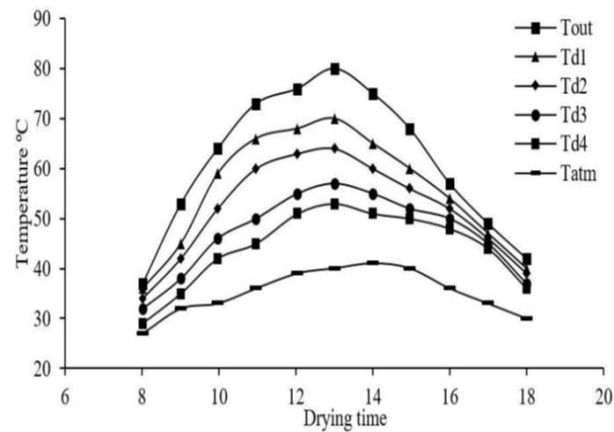


Fig (II-12): Diurnal variation of the collector outlet air temperature, Temperature above each tray and atmospheric air temperature for the natural convection Solar dryer for sample load conditions.

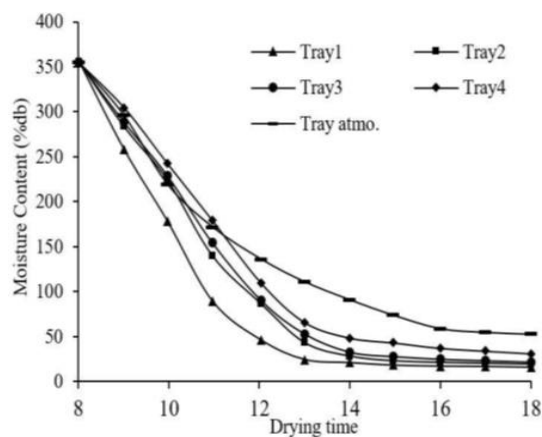


Fig (II-13): Drying time vs moisture content

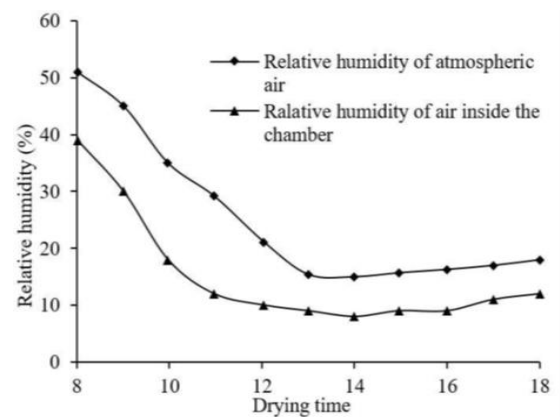


Fig (II-14): Drying time vs relative humidity

M. I. Fadhel et al [6] :

In this work, an experimental study was performed to determine the thin layer drying characteristics of banana slices in a force convection indirect solar drying. During the experiments, the cabinet was loaded with 426g of banana slices having an initial moisture content of 80%. In this study eight different thin layer-drying models were compared, the performance of these models was investigated by non-linear regression analysis using statistical computer program. The entire models were showed a good fit to the drying data. However, the (wang and singh) drying model was showed a better fit to the experiment data among other models.



Fig (II-15): Picture of indirect forced circulation solar drying thermal system.

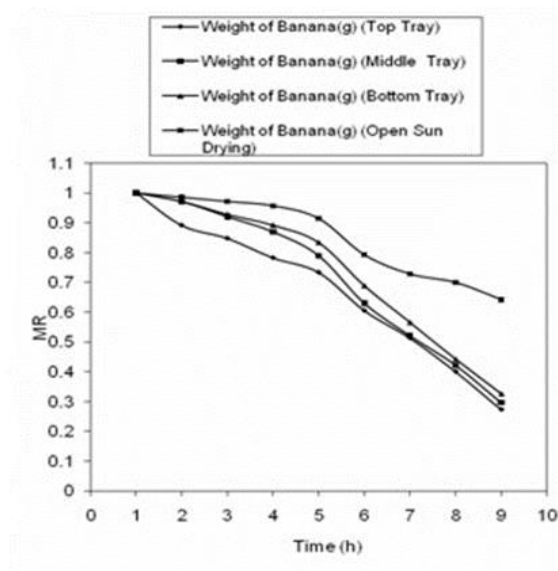


Fig (II-16): Moisture ratio versus Time (h) curves.

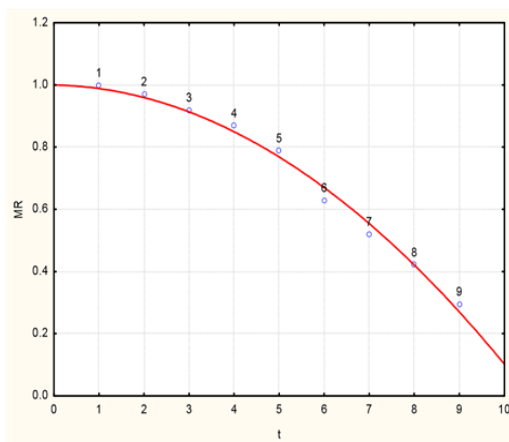


Fig (II-17): Wang and Singh model drying curve (Middle tray).

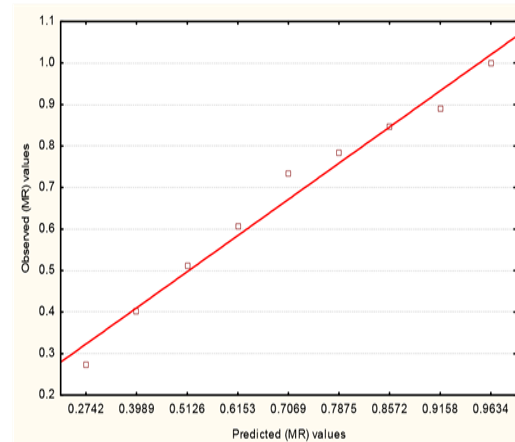


Fig (II-18): Wang and Singh model (Middle tray) Observed moisture content versus predicted moisture ratio for banana slice.

Fahim Ullah et al [7]:

The aim of this work was to study the drying behavior of Asparagus by using a natural convection indirect solar dryer, the experiments were conducted during the months of June, July, and August 2016, at College of Engineering, Nanjing Agricultural University, Nanjing, China.

In this study a Linear regression method was applied to the experimental data to evaluate the Nusselt number constant, from the results of the experiment, it was reported that moisture removing rate increased with the increase in mass of asparagus samples and significantly decreased with progression of drying months.



Fig (II-19): Asparagus samples before drying (a) and after drying (b)

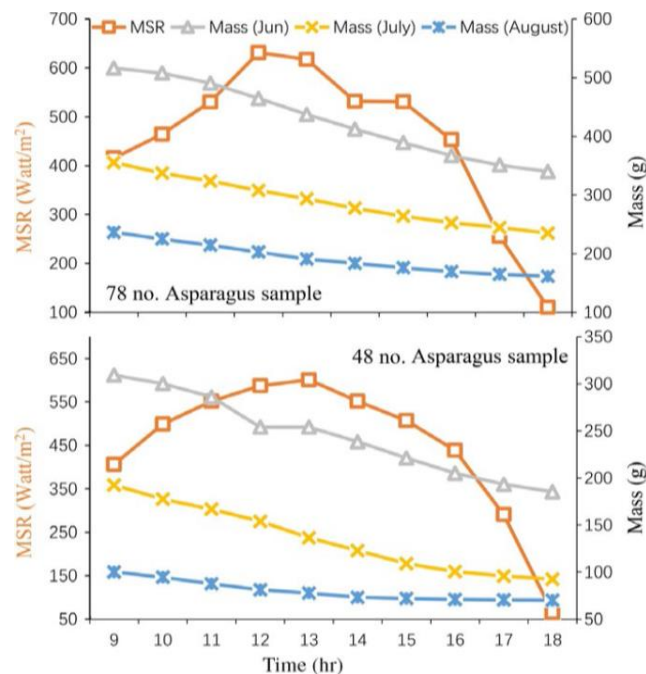


Fig (II-20) : The variation of solar irradiation and mass of the product with respect to time for 78 and 48 no of asparagus samples ; MSR shows the mean solar irradiance in W/m^2 for the 3 months, that is, Jun, July, and August ; Mass (Jun, July, and August) is the mass of the product of both 78 and 48 No. Samples of asparagus.

S. Prakash et al [8]:

This work was aimed to study the drying characteristics of carrots using a solar cabinet dryer, fluidized bed dryer and microwave oven dryer. Drying occurred mainly in the falling rate period. Carrots dried by fluidized bed drying showed better colour, rehydration properties, greater b-carotene retention and better overall sensory acceptability than those dried by microwave oven and solar cabinet dryer.

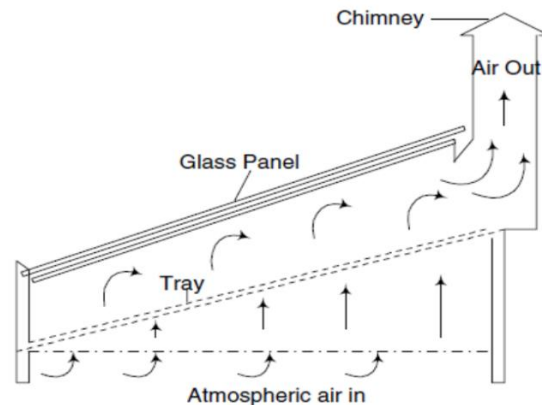


Fig (II-21): schematic diagram of solar cabinet dryer.

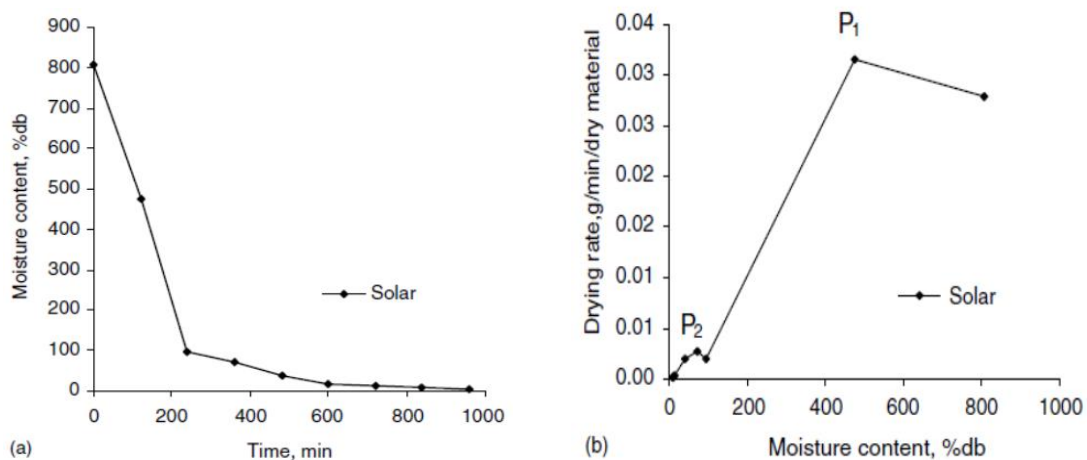


Fig (II-22): (a) moisture content vs time for solar cabinet dryer and (b) drying rate vs moisture Content for solar cabinet dryer.

Shahrbanou Shamekhi-Amiria et al [9]:

The aim of this study was to investigate the thin-layer drying behaviour of lemon balm leaves in an indirect-mode solar dryer with forced convection, by using a solar air heater with double-pass packed bed of wire mesh layer configuration to enhance the energy gain of the heated air.

Their drying experiments were performed for lemon balm leaves with initial moisture content of 80% on wet basis to the final moisture content of 10%. They also tested a Mathematical models to find the best thin layer model for describing the drying behaviour of lemon balm leaves.



Fig (II-23): Photo of the tested solar dryer. **Fig (II-24):** The final dried product.

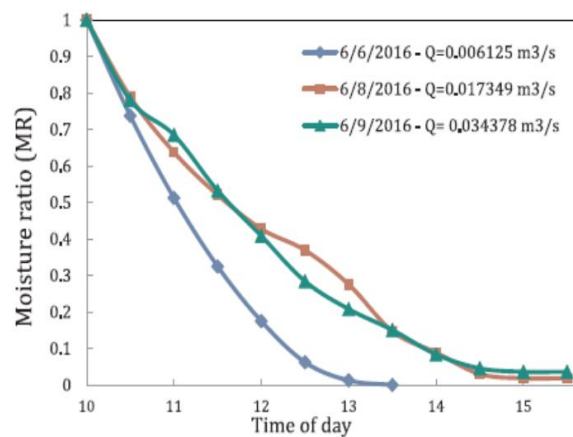


Fig (II-25): Variation of moisture ratio versus drying time depicted at various airflow rates on different days.

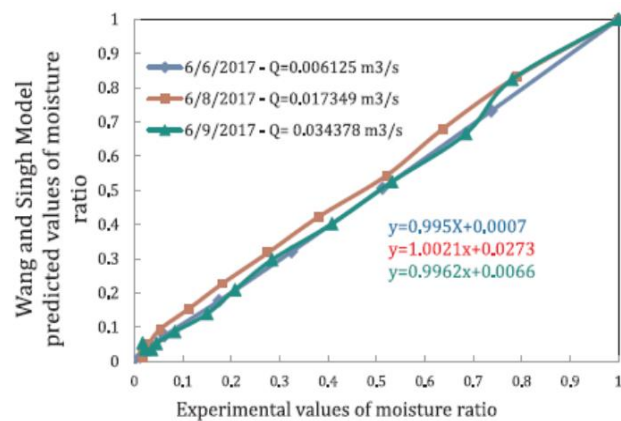


Fig (II-26): Comparison between experimental moisture ratios and that predicted for Lemon blam calculated using the wang and singh model.

Samira Chouicha et al [10]:

In this work, they studied the solar hybrid drying of sliced potatoes by forced convection in indirect solar dryer using extra energy via a heater by joule effect generated by photovoltaic modules connected in parallel. The main results show that:

Hybrid drying (solar energy) with improving the delivery of solar panels, drying time and quality of the product. Used operating conditions were air flow speed 0.51 m/s in duration of 2h 45min through the period between Mai 06th, 2012 and Mai 28th, 2012.

Hybrid drying (conventional electric power) using a maximum speed, performed at : 0.5 m/s in duration of 1 h 15min through the period between Mai 13th, 2012 to Mai 18th, 2012.



Fig (II-27): Schematic of the drying system.

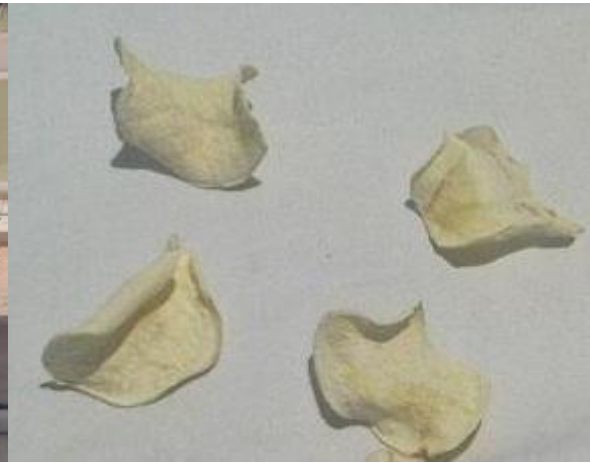


Fig (II-28): Visual quality of the dried potato.

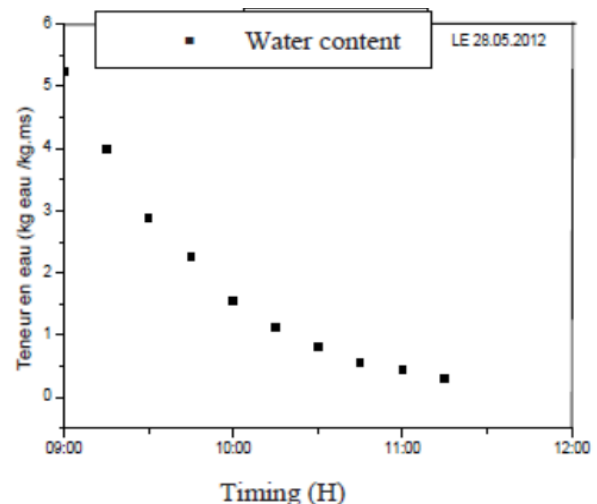
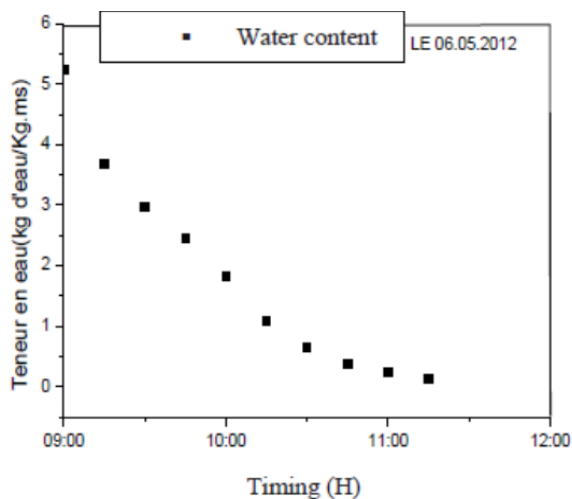


Fig (II-29): variation of water content as function of time associated with one panel (a) and two panels (b).

S. K. Sansaniwal and M. Kumar et al [11]:

Their work present, a study of drying behaviour of ginger rhizomes by using a natural convection indirect solar dryer, the various experiments were conducted during the months of March and April 2014 at Guru Jambheshwar University of Science and Technology, India.

The experimental data were analysed by using Nusselt number expression with the help of linear regression method. The moisture removing rate on dry basis for each drying hour was evaluated and observed to be increased with increase in ginger samples mass and decreases significantly with the progression of drying days, and the convective heat transfer coefficients for both mass of ginger samples decrease significantly with increase in the mass of ginger samples.



Fig (II-30): pictorial view of the solar drying system.



Fig (II-31): Ginger samples (a) before drying; (b) after drying.

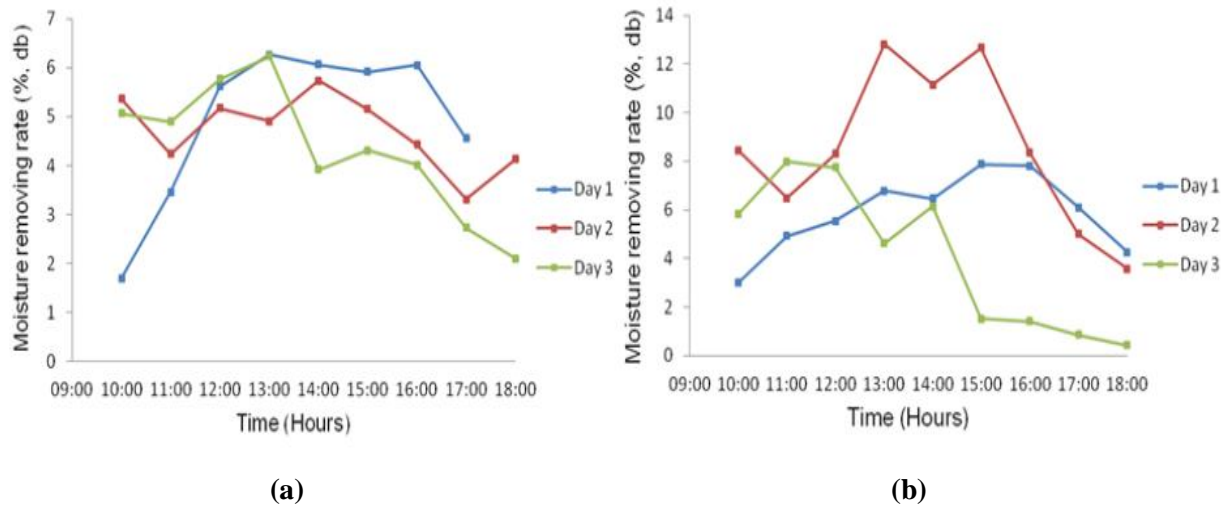


Fig (II-32): Variations in moisture removing rate (% , dry basis) with respect to time (a) for 78 no, of ginger samples (b) for 48 no, of ginger samples.

H. Samimi. Akhijani et al [12]:

In this presented work, a mathematical modelling and effective moisture diffusivity of tomato was studied during hot air solar drying. Drying experiments were performed in a thin layer hot air drying at slice thicknesses of 3, 5 and 7 mm and air velocities of 0.5, 1 and 2 m/s.

The experimental data were fitted to different mathematical moisture ratio models and the Page model was selected as the best model. The maximum values of moisture diffusivity was 6.98×10^{-9} m²/s at air velocity of 2 m/s and slice thickness of 7 mm while the minimum value of the moisture diffusivity was 1.58×10^{-9} m²/s at air velocity of 0.5 m/s and slice thickness of 3 mm.

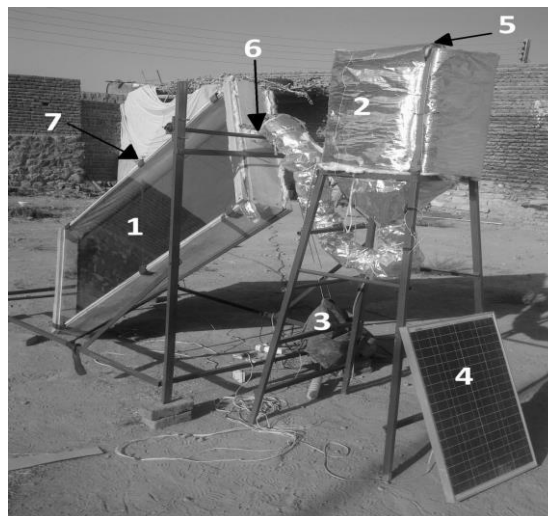


Fig (II-33): The laboratory scale of the solar swivel dryer.

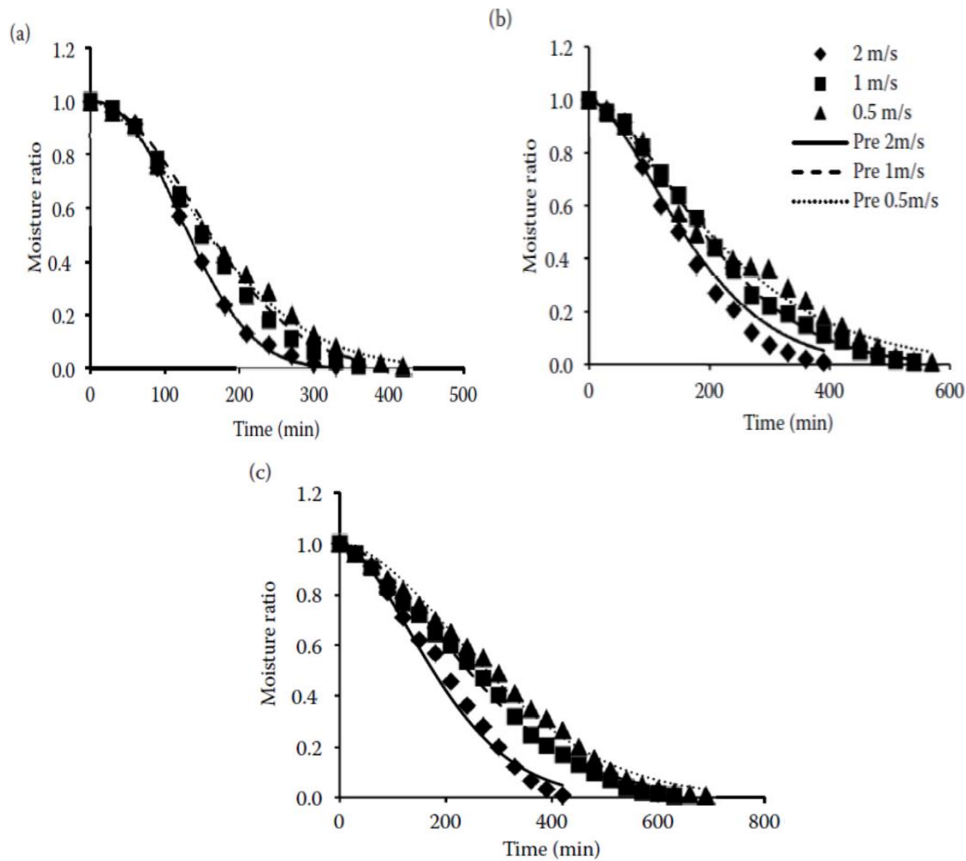


Fig (II-34): drying of tomato slices 3, 5 and 7 mm and fitted curves (a) (b) (c) of the page model.

Mohamed Yacine Nasri et al [13]:

In this study, the experiments were carried out on solar drying of potatoes, cut in three different shapes; cylindrical, cubical and rectangular parallelepipedic, with same quantity, and Using the diffusion model and experimental curves of the drying kinetics. The results show that, the drying kinetics depend, on the shape and the size of items, which constitute each quantity.

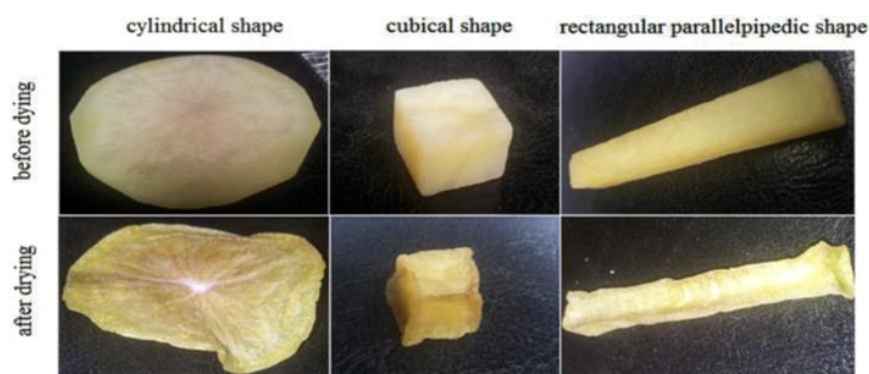


Fig (II-35): Shape at the beginning and the end of drying.



Fig (II-36): The experimental solar dryer.



Fig (II-37): Products disposition for the first experimental set.

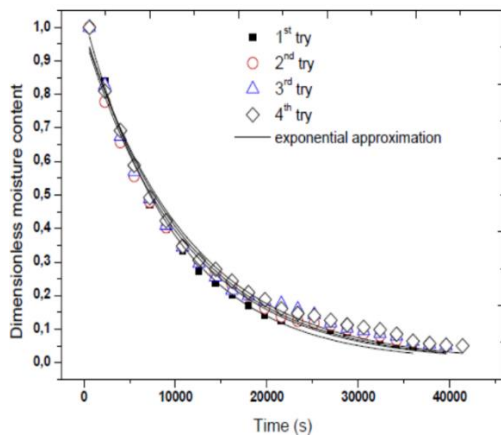


Fig (II-38): Experimental with exponential approximation average dimensionless moisture ratio vs drying time for the four try of cube shape.

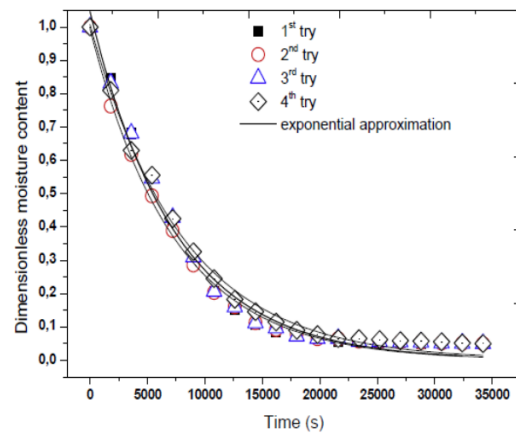


Fig (II-39): Experimental with exponential approximation average dimensionless moisture ratio vs drying time for the four try of disc shape.

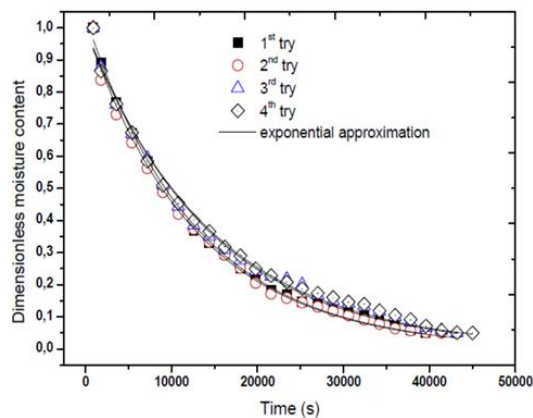


Fig (II-40): Experimental with exponential approximation average dimensionless moisture ratio vs drying time for the four try of parallepipedic shape.

P.P. Tripathy et al [14]:

In this presented work, a natural convection mixed-mode solar dryer is used for performing the experiments on potato cylinders and slices with same thickness of 0.01 m with respective length and diameter of 0.05 m. for determination of convective heat transfer coefficient. The present investigation indicates that the cylindrical samples exhibit higher values of h_c and faster drying rate compared to those of slices. Results of energy analysis reveal that for both the sample geometries, decreasing product moisture content during drying resulted in significant reduction in specific energy consumption. For almost similar drying conditions, a considerable amount of reduction in specific energy consumption is achieved for cylinders, as expected.

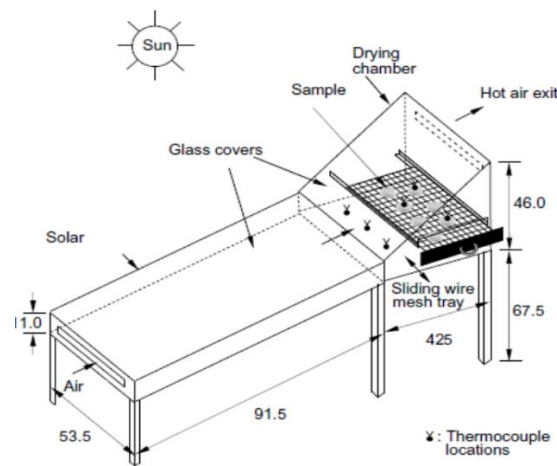


Fig (II-41): Schematic diagram of the mixed-mode solar dryer. (The dimensions are in cm.)

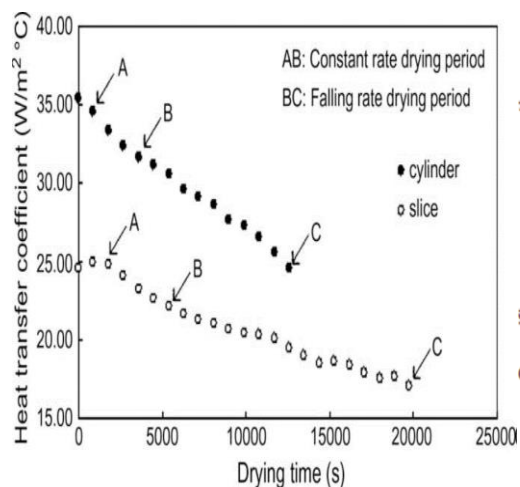


Fig (II-42): Variation of convective heat transfer coefficient with drying time for potato cylinders and slices.

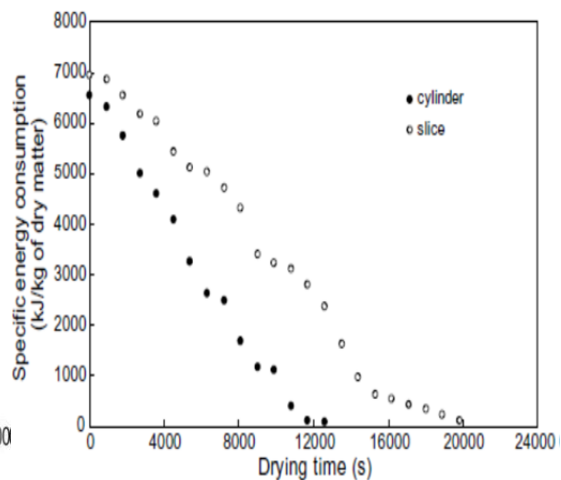


Fig (II-43): Variation of specific energy consumption with drying time for potato cylinders and slices.

Y.I. Sallam et al [15]:

In this study, two identical prototypes direct and indirect solar dryers were used to dry whole mint under natural and forced convection, to investigate the effect of flow mode and the type of solar dryers on the drying kinetics of whole mint. The results indicated that drying of mint under different operating conditions occurred in the falling rate period, where no constant rate period of drying was observed. Also, the obtained data revealed that the drying rate of mint under forced convection was higher than that of mint under natural convection, especially during first hours of drying (first day).



Fig (II-44): Photograph of the direct solar dryer.

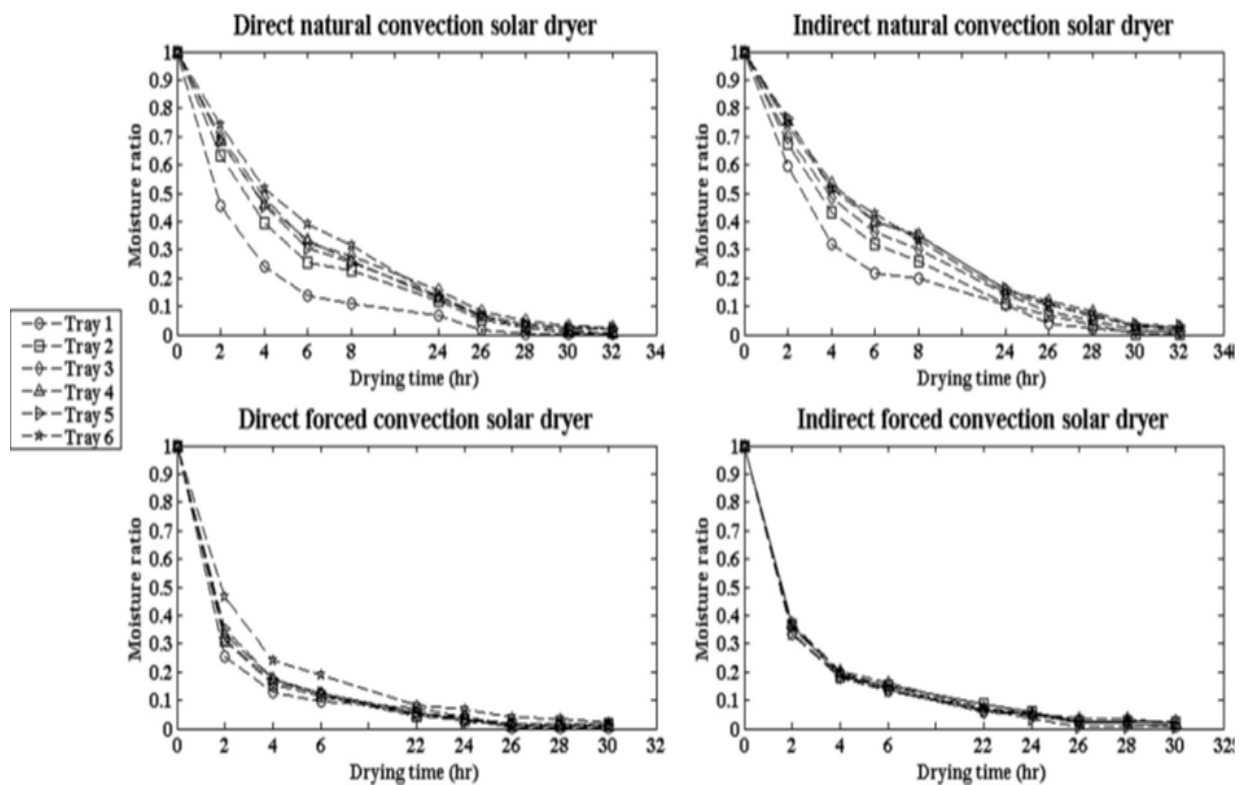


Fig (II-45): Variation in the mint moisture ratio with drying time.

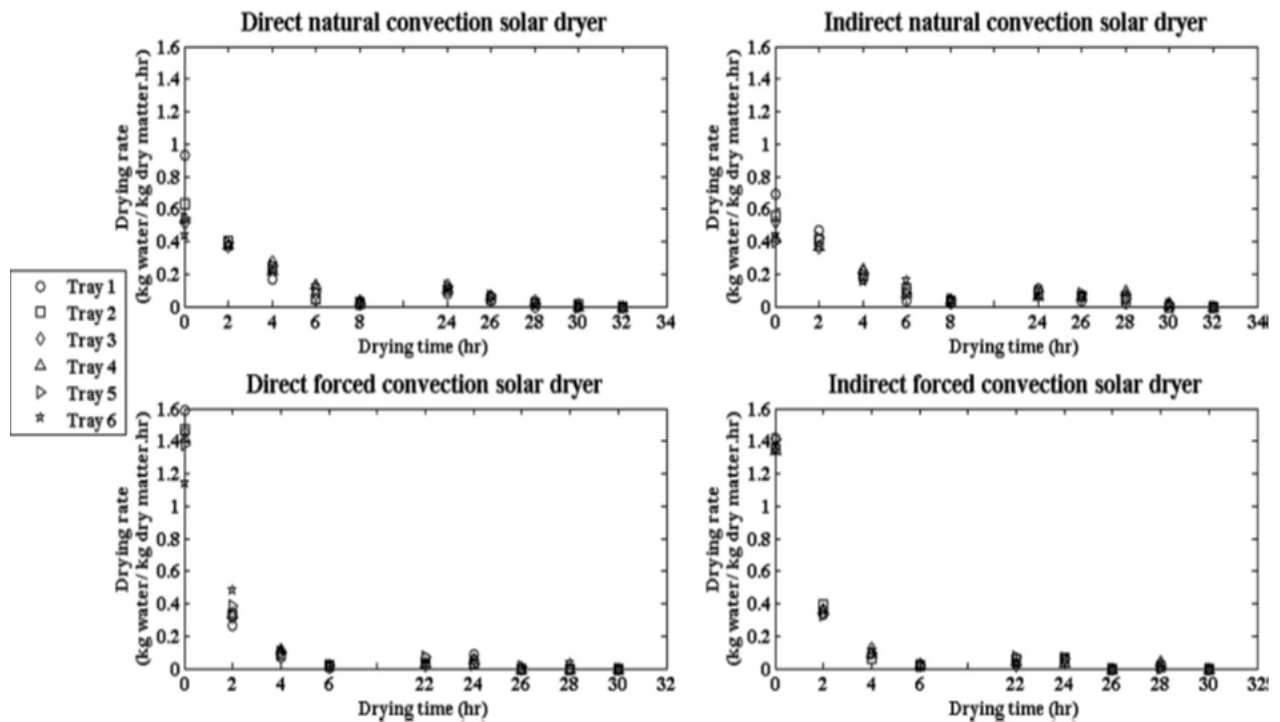


Fig (II-46): Variation in the mint-drying rate with drying time.

II.3. Conclusion:

After taking a look on these previous studies that have been carried out on the solar drying of agricultural products. We can say that these studies can be developed and improved by using many techniques as needed, so for that, researchers are always looking for ameliorate the drying yield by the possible ways, they also depend on a several mathematical models to compare their studies with, and the purpose of all these is getting the best quality and reducing the drying time.

«References»

- [1]: Pangavhane, Dilip R., R. L. Sawhney, and P. N. Sarsavadia. "Design, development and performance testing of a new natural convection solar dryer." *Energy* 27.6 (2002): 579-590.
- [2]: Abdel-Galil, H. S., and A. A. El-Nakib. "EFFECT OF NUTURAL CONVECTION SOLAR DRYING ON QUALITY OF PEPPERMINT."
- [3]: Ayadi, M., I. Zouari, and A. Bellagi. "Simulation and Performance of a Solar Drying Unit with Storage for Aromatic and Medicinal Plants." *International journal of food engineering* 11.5 (2015): 597-607.
- [4]: Nabhan Al khuresi, Santosh Walke. "Drying Characteristics of Fruits using Solar Drying." *International Journal of Emerging Technologies and Engineering* (2016): 2348 – 8050.
- [5]: Lingayat, Abhay, V. P. Chandramohan, and V. R. K. Raju. "Design, development and performance of indirect type solar dryer for banana drying." *Energy Procedia* 109 (2017): 409-416.
- [6]: Fadhel, M. I., et al. "Thin-layer drying characteristics of banana slices in a force convection indirect solar drying." *Proceedings of the 6th IASME/WSEAS International Conference on Energy and Environment (EE 2011)*. World Scientific and Engineering Academy and Society Press, 2011.
- [7]: Ullah, Fahim, et al. "Retracted: Experimentally investigated the asparagus (*Asparagus officinalis* L) drying with flat-plate collector under the natural convection indirect solar dryer." *Food Science & Nutrition* 6.6 (2018): 1357-1357.
- [8]: Prakash, S., S. K. Jha, and Nivedita Datta. "Performance evaluation of blanched carrots dried by three different driers." *Journal of Food Engineering* 62.3 (2004): 305-313.
- [9]: Shamekhi-Amiri, Shahrbanou, et al. "Drying behaviour of lemon balm leaves in an indirect double-pass packed bed forced convection solar dryer system." *Case studies in thermal engineering* 12 (2018): 677-686.
- [10]: Chouicha, Samira, et al. "Solar drying of sliced potatoes. An experimental investigation." *Energy Procedia* 36 (2013): 1276-1285.
- [11]: Sansaniwal, S. K., and M. Kumar. "Analysis of ginger drying inside a natural convection indirect solar dryer: An experimental study." *Journal of Mechanical Engineering and Sciences* 9.unknown (2015): 1671-1685.

[12]: Akhijani, H. Samimi, A. Arabhosseini, and M. H. Kianmehr. "Effective moisture diffusivity during hot air solar drying of tomato slices." *Research in Agricultural Engineering* 62.1 (2016): 15-23.

[13]: Nasri, Mohamed Yacine, and Azeddine Belhamri. "Effects of the climatic conditions and the shape on the drying kinetics, Application to solar drying of potato-case of Maghreb's region." *Journal of cleaner production* 183 (2018): 1241-1251.

[14]: Tripathy, P. P., and Subodh Kumar. "Modeling of heat transfer and energy analysis of potato slices and cylinders during solar drying." *Applied Thermal Engineering* 29.5-6 (2009): 884-891.

[15]: Sallam, Y. I., et al. "Solar drying of whole mint plant under natural and forced convection." *Journal of advanced research* 6.2 (2015) : 171-178.

Chapter III

Experimental

and

theoretical study

III.1. Introduction:

Solar drying is one of the processes that have found application in Algeria, because of the important quantities of solar irradiations that can be exploited in this country, and the main purpose of this process is to conserve the agricultural products for use it in any time.

This chapter is aimed to describe the solar drying behaviour of some agricultural products by using an indirect solar dryer, designed and constructed previously. Also, mathematical models were used for describing this operation based on the experiment data. The experiments took place at the University of Biskra and have been carried out between February and April 2019.

III.2. Experiments location and zone climate:

III.2.1. Experiments location:

The experiments were carried out near the technological hall of mechanical engineering department from university of Biskra, which is located at latitude $34^{\circ}48'$ and longitude $5^{\circ}44'$, in the south-east of Algeria with 120 m of altitude in relation to the level of the sea, the city lies about 400 klm from Algiers.



Fig (III-1): Satellite picture of the experience area.

III.2.2. Experiments zone climate:

Biskra takes place in the arid region, it is characterized by a very hot and dry summer; the average temperature is 43.5 °C with 12% of relative humidity in the average, and a very cold winter; average minimum temperature of 4 °C with an average maximum relative humidity of 89% [1].

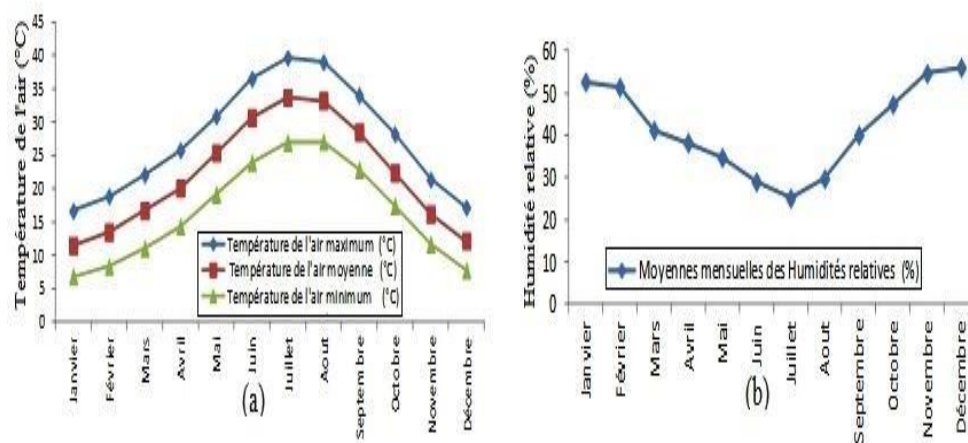


Fig (III-2): Temperature and relative humidity curves of Biskra [1].

III.3. Experimental study:

In this study, we focused on agro-food drying, using a solar collector and a drying chamber, which designed and constructed previously in the technological hall of mechanical engineering department from university of Biskra, carried out in the period from February to April 2019.



Fig (III-3): Experimental setup (solar collector with drying chamber).

III.3.1. Manufacture of the drying chamber:

The room is made of multiple type wood, protected on all sides with good quality insulation. Connect to the solar panel by a pipe, which passes air through holes to distribute this air on the dried product; its dimensions are 80cm x 50cm x 50cm.



Fig (III-4): Experimental setup of drying chamber.

- **Orifices:** We drilled holes in order to distribute the air on the product and avoid burning it. In our case, we put holes 10 mm in diameter in a square board, 30 cm by 30 cm. As shown in figure (III-5).

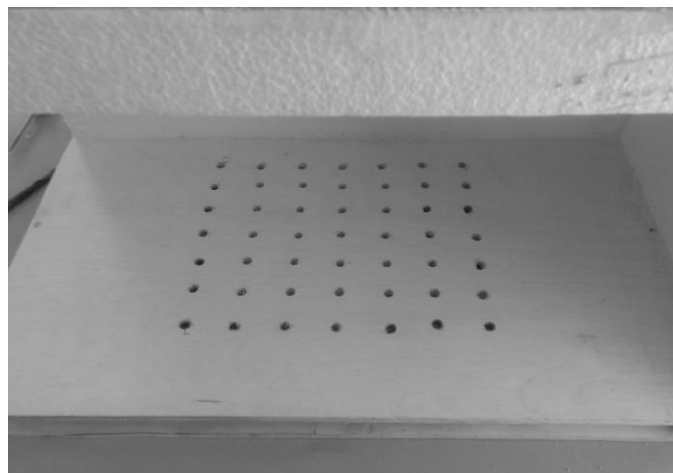


Fig (III-5): Orifices into drying chamber.

- **The grate:** Is a support on which the product is arranged, with holes for the removal of water, attached by four rods equilibrated to allow us to weigh the product without removing it, see Fig (III-6). This grid is characterized by its hardness and resistance to rust.



Fig (III-6): Support of the drying product.

III.3.2. The balance system modification:

Before starting with the principle experiments, we have done a test on our solar dryer to see how much it is ready for the drying operation, a problem has been found on the balance system, it was very heavy and unstable, because of that, the electronic balance did not give us accurate values.

This system is suspended by the electronic balance and consist of two rectangular metallic mesh plates, one in the outside and the other one in the inside of drying room and connected by four metallic wires as shown in the figure (III-7).

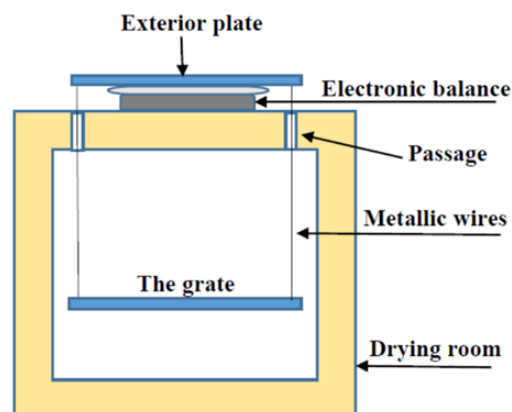


Fig (III-7): Schematic view of balance system.

The main problem was in the friction between the metallic wires and their passages because they were not exactly parallel. So after thinking about a suitable solution we suggested to use monofilament (thread of fishing) as an alternative to the metallic wires and changing the exterior metallic plate by a wooden one, see figure (III-8), this solution was very positive it allowed us to reduce the friction completely and facilitate the extraction of values.



Fig (III-8): The balance system modifications.

III.3.3. Experimental Procedure:

Experimental observations were recorded between 9:00 am to 16:30 pm during the month of February and April 2019 at the University of Biskra. Three different sizes of the thin layer of slices of potato, carrot and apple such as 1, 1.5, 2 and 3 mm, were placed on a rectangular shaped wire mesh plates, which were used to accommodate different mass of our samples. These plates were taken on the digital electronic balance machine to determine the moisture content removal for each drying half hour, see figure (III-9).



Fig (III-9): A digital electronic balance machine.

A thermometer-control (Model TPM-10) see Fig (III-10), was kept just above the slice of the product surface to measure the temperature and the humidity.



Fig (III-10): A thermometer-control (Model TPM-10).

The temperature was measured by using calibrated thermocouples type k as shown in figure (III-11), at different locations, namely dryer inlet temperature, product surface temperature, drying room inlet and outlet temperature, solar collector inlet and outlet temperature and absorbing plate temperature of the collector.



Fig (III-11): A thermocouples type k.

An Hygrometer (Model PCE-555) used to measure the relative humidity of the exterior.



Fig (III-12): Hygrometer (Model PCE-555).

A pyranometer (Model Voltcraft PL-110SM) robust and easy to use device for measuring the intensity of solar radiation per unit of W/m^2 as shown in figure (III-13).



Fig (III-13): pyranometer (Model Voltcraft PL-110SM).

A digital anemometer (Model KIMO-LVA) see figure (III-14), having a readability of 0.01 m/s was used to measure the wind velocity.



Fig (III-14): A digital anemometer (Model KIMO-LVA).

The experimental observations were recorded in every 30 minutes time interval. The measurement was discontinued when the constant mass of samples was completed. The difference in mass directly gave the quantity of water content evaporated during any time interval. These three different products have a diameter of 44mm, 30mm for potato and carrot respectively and 32mm of radius for apple. Wet and dried potato, carrot and apple are shown in the figures (III-12), (III-13) and (III-14) respectively.



Fig (III-12): Wet and dried slices of potato with 1mm of thickness and 44 mm of diameter.

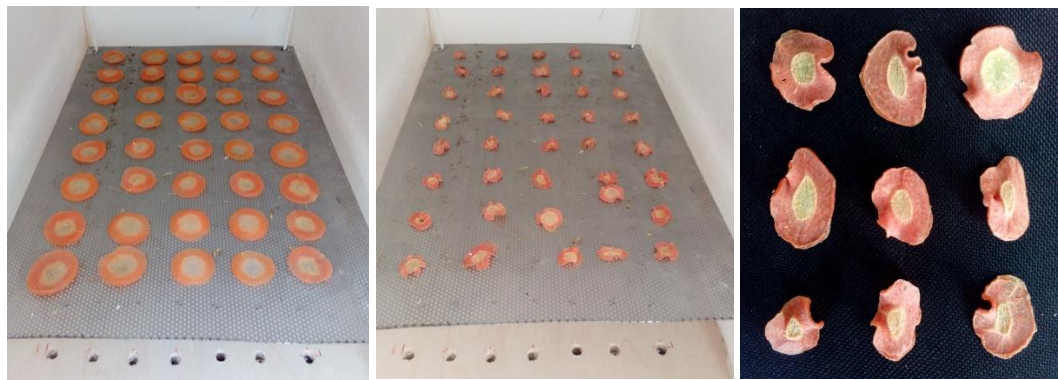


Fig (III-13): Wet and dried slices of carrot with 1mm of thickness and 30mm of diameter.



Fig (III-14): Wet and dried slices of apple with 1mm of thickness and 32mm of radius.

III.4. Theoretical study:

The moisture content was expressed in percentage wet basis (% w.b) and then converted to kilogram water per kilogram dry matter. The drying curves were fitted to three different moisture ratio models to select a suitable model for describing the drying process of slice potato pieces (Table III-1).

Models	Equation	References
Newton	$MR = \exp(-k \cdot x)$	(Ayensu, 1997) [2]
Henderson and Pabis	$MR = a \exp(-kt)$	(Rahman et al. 1998) [3]
Logarithmic	$MR = a \exp(-kt) + c$	(Lahsasni et al. 2004) [4]

Table (III-1): Mathematical model applied to the drying curves

The moisture ratio of the samples during drying was expressed by the Equation (III-1):

$$MR = \frac{M_t - M_{eq}}{M_0 - M_{eq}} \quad \text{(III-1)}$$

Where (M_t) is the moisture content at any drying time (% , wet basis), (M_0) is the initial moisture content (% , wet basis), and (M_{eq}) is the equilibrium moisture content (% , wet basis).

However, the moisture ratio (MR) was simplified by modifying the Equation (1) to $\frac{M_t}{M_0}$ instead

of the $\frac{M_t - M_{eq}}{M_0 - M_{eq}}$ [5].

The reduced chi-square χ^2 and root mean square error ($RMSE$) were used as the primary criterion to select the best equation to account for variation in the drying curves of the dried samples [6]. The model suitability was determined by considering the highest value of coefficient of determination and least value of chi square and root mean square error.

The statistical values were calculated by Equations (III-2), (III-3) and (III-4):

$$\chi^2 = \frac{\sum_{i=1}^N (M_{\text{exp}i} - M_{\text{mod}i})^2}{N - m} \quad \text{(III-2)}$$

$$RMSE = \left(\frac{1}{N} \sum_{i=1}^N (M_{\text{exp}i} - M_{\text{mod}i})^2 \right)^{\frac{1}{2}} \quad \text{(III-3)}$$

$$SSE = \frac{1}{N} \sum_{i=1}^N (M_{\text{exp}i} - M_{\text{mod}i})^2 \quad \text{(III-4)}$$

$$R^2 = \frac{\sum_{i=1}^N (M_{\text{exp}i} - M_{\text{mod}i}) \sum_{i=1}^N (M_{\text{mod}i} - M_{\text{exp}i})}{\sqrt{\left[\sum_{i=1}^N (M_{\text{exp}i} - M_{\text{mod}i})^2 \right] \left[\sum_{i=1}^N (M_{\text{mod}i} - M_{\text{exp}i})^2 \right]}} \quad \text{(III-5)}$$

Where ($M_{\text{exp},i}$) is the experimental moisture ratio, ($M_{\text{mod},i}$) is the predicated moisture ratio, (N) is the number of observations, and (m) is the number of drying model constant.

III.4.1. Calculation of effective diffusivities:

It has been accepted that the drying characteristics of biological products in the falling rate period can be described by using Fick's diffusion equation. The solution of Fick's law for a slab was, according to Equation (III-5) [7].

$$\frac{M_t - M_{eq}}{M_0 - M_{eq}} = \frac{8}{\pi^2} \sum_{n=1}^{\infty} \frac{1}{(2n+1)^2} \exp\left(- (2n+1)^2 \pi^2 \frac{D_{eff} t}{4H^2}\right) \quad (\text{III-5})$$

For a long drying period, Equation (III-5) can be further simplified to only the first term of the series [8]. Thus, Equation (III-5) is written in a logarithmic form according to Equation (III-6):

$$\ln \frac{M_t - M_{eq}}{M_0 - M_{eq}} = \ln\left(\frac{8}{\pi^2}\right) - \left(\pi^2 \frac{D_{eff}}{4H^2}\right) t \quad (\text{III-6})$$

Diffusivities are typically determined by plotting experimental drying data in terms of Ln (MR) versus drying time t in Equation (III-6), because the plot gives a straight line with a slope according to Equation (III-7) [9].

$$k_0 = \left(\pi^2 \frac{D_{eff}}{4H^2}\right) \quad (\text{III-7})$$

III.4.2. Thin layer drying model:

In order to describe the solar drying behaviour of the thin layer drying process with three different agricultural products, we decided to find and define a mathematical model to determine the moisture ratio MR as a function of the drying time by using the obtained experimental data.

This model was chosen by non-linear equation (III-8), and to compute its constants (a and b) it must be transformed into a linear equation and using the least square method to find these constants. This model was evaluated to be a good fit based on the correlation coefficient R^2 and the approximation with experimental curves.

$$MR = a \times b^t \quad (\text{III-8})$$

III.4.3. Least Squares method:

Least squares is a statistical method used to determine a line of best fit by minimizing the sum of squares created by a mathematical function see fig (III-15). A "square" is determined by squaring the distance between a data point and the regression line or mean value of the data set.

The least squares approach limits the distance between a function and the data points that a function is trying to explain. It is used in regression analysis, often in nonlinear regression modeling in which a curve is fit into a set of data [10].

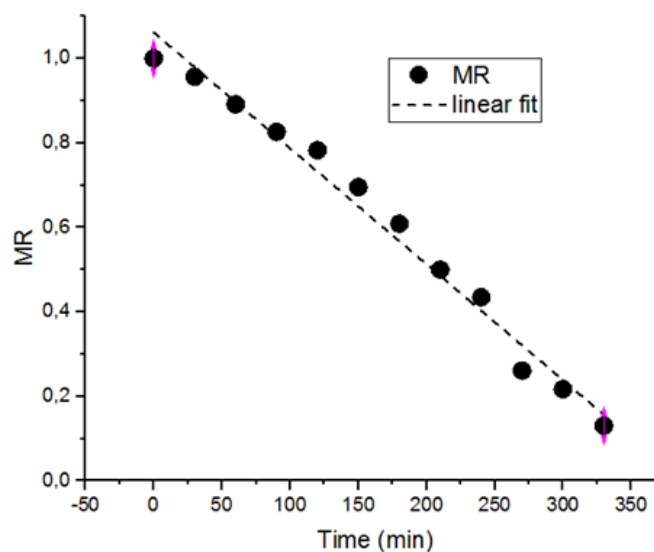


Fig (III-15): Example of linear fitting.

III.4.4. Linearization of Nonlinear Behavior:

As we said before our model has a form of non-linear equation, and it must be transformed into linear equation because the linear regression is useful to represent a linear relationship. So we could transform this kind of equations into linear equation as follows:

Generally, the equation is written as:

$$y = ab^x \quad (\text{III-9})$$

Taking logarithm of both sides of eq (III-9):

$$\ln y = \ln a + x \ln b \quad (\text{III-10})$$

This is in form of a linear equation:

$$y' = \alpha + \beta x \quad (\text{III-11})$$

Where:

$$y' = \ln y$$

$$\alpha = \ln a$$

$$\beta = \ln b$$

In our case that related to the moisture ratio, equations are written as:

$$MR = ab^t$$

$$\ln MR = \ln a + t \ln b$$

$$y' = \alpha + \beta t$$

Where:

$$y' = \ln MR$$

$$\alpha = \ln a$$

$$\beta = \ln b$$

III.4.5. Determination of the model constants:

Determine on the unknowns constants (a) and (b) by minimizing the sum of squares of the residuals (Sr), and to do this set the derivatives of Sr with (α) and (β) to zero:

$$Sr = \sum_{i=1}^n (y'_i - \alpha - \beta t_i)^2 \quad (\text{III-12})$$

$$\frac{\partial Sr}{\partial \alpha} = -2 \sum_{i=1}^n (y'_i - \alpha - \beta t_i) = 0 \quad (\text{III-13})$$

$$\frac{\partial Sr}{\partial \beta} = -2 \sum_{i=1}^n [(y'_i - \alpha - \beta t_i) t_i] = 0 \quad (\text{III-14})$$

Equations (III-13) and (III-14) lead to the equations:

$$\rightarrow n\alpha + \left(\sum t_i\right)\beta = \sum y_i' \quad \text{(III-15)}$$

$$\rightarrow \left(\sum t_i\right)\alpha + \left(\sum t_i^2\right)\beta = \sum t_i y_i' \quad \text{(III-16)}$$

In matrix form,

$$\begin{bmatrix} n & \sum t_i \\ \sum t_i & \sum t_i^2 \end{bmatrix} \begin{bmatrix} \alpha \\ \beta \end{bmatrix} = \begin{Bmatrix} \sum y_i' \\ \sum t_i y_i' \end{Bmatrix} \quad \text{(III-17)}$$

After solving these, we can find the unknowns constants:

$$\beta = \frac{n \sum (t_i y_i') - \sum t_i \sum y_i'}{n \sum t_i^2 - (\sum t_i)^2} \quad \text{(III-18)}$$

$$\alpha = \bar{y} - \beta \bar{t} \quad \text{(III-19)}$$

Where \bar{y} and \bar{t} are the means of y and t, respectively.

$$\bar{y} = \frac{1}{n} \sum y_i'$$

$$\bar{t} = \frac{1}{n} \sum t_i$$

III.4.6. Application of the least square method:

After seen how to find and determine the unknown constants of the non-linear equation by using the least square method, now we are going to show the application of this method by using two different programs; the first one by using Microsoft Excel and the second one by using Matlab program, the explanation is shown below.

III.4.6.1. Example of Microsoft Excel:

To calculate the unknown constants (a and b) and the factor of determination R^2 , we suggested to make a program by using Microsoft Office Excel, which is based on the obtained experimental data and the necessary correlations, see fig (III-16).

	t	MR	ln(MR)	t ²	ln(MR) ²	t*ln(MR)
	0	1	0	0	0	0
	30	0,93181818	-0,07061757	900	0,00498684	-2,11852702
	60	0,81818182	-0,2006707	3600	0,04026873	-12,0402417
	90	0,72727273	-0,31845373	8100	0,10141278	-28,6608358
	120	0,59090909	-0,5260931	14400	0,27677395	-63,1311715
	150	0,43181818	-0,83975065	22500	0,70518116	-125,962598
	180	0,27272727	-1,29928298	32400	1,68813627	-233,870937
	210	0,13636364	-1,99243016	44100	3,96977796	-418,410335
	240	0,02272727	-3,78418963	57600	14,3200912	-908,205512
Sx	1080					
Sy	-9,03148853					
Sxy	-1792,40016					
Sxx	183600					
Syy	21,1066289					
ym	-1,00349873					
xm	120					
ln(b)	=		-0,01312262	b	0,992	
ln(a)	=		0,5712158	a	1,1553	
R	=		-0,87869945	R ²	0,915	

Fig (III-16): Calculation of a, b, R² by using Microsoft Excel.

Where:

R is the correlation coefficient and R² is the factor of determination

$$R = \frac{n \sum (t_i y_i') - \sum t_i \sum y_i'}{\sqrt{n \sum t_i^2 - (\sum x_i)^2} \sqrt{n \sum y_i'^2 - (\sum y_i')^2}}$$

$$sx = (\sum t_i), \quad sy = (\sum \ln MR)$$

$$sxy = (\sum t_i \cdot \ln MR), \quad sxx = (\sum t_i)^2$$

$$syy = (\sum \ln MR)^2$$

$$xm = \bar{t} = \frac{1}{n} \sum t_i$$

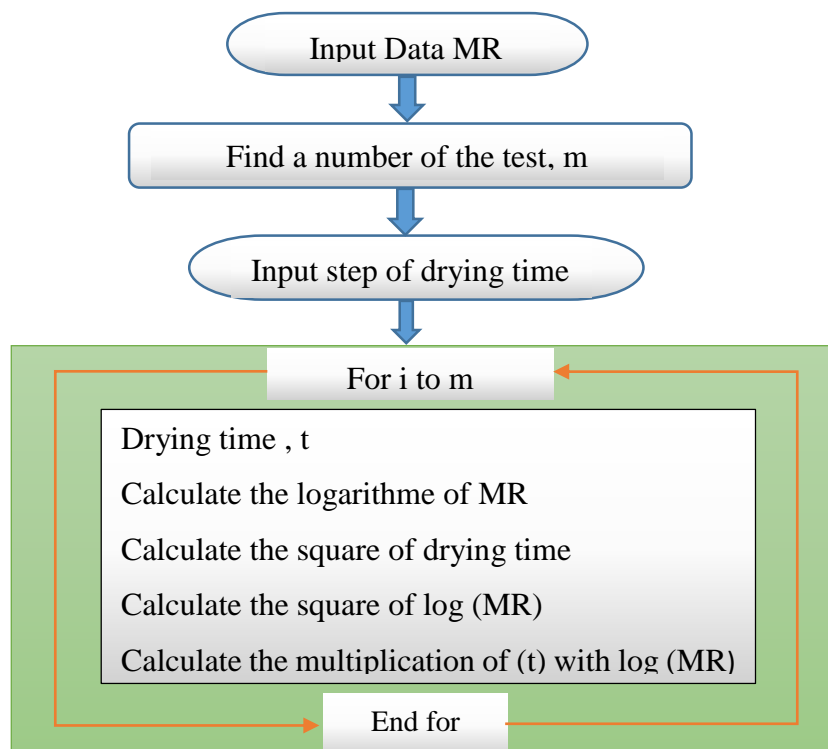
$$ym = \bar{y} = \frac{1}{n} \sum y_i'$$

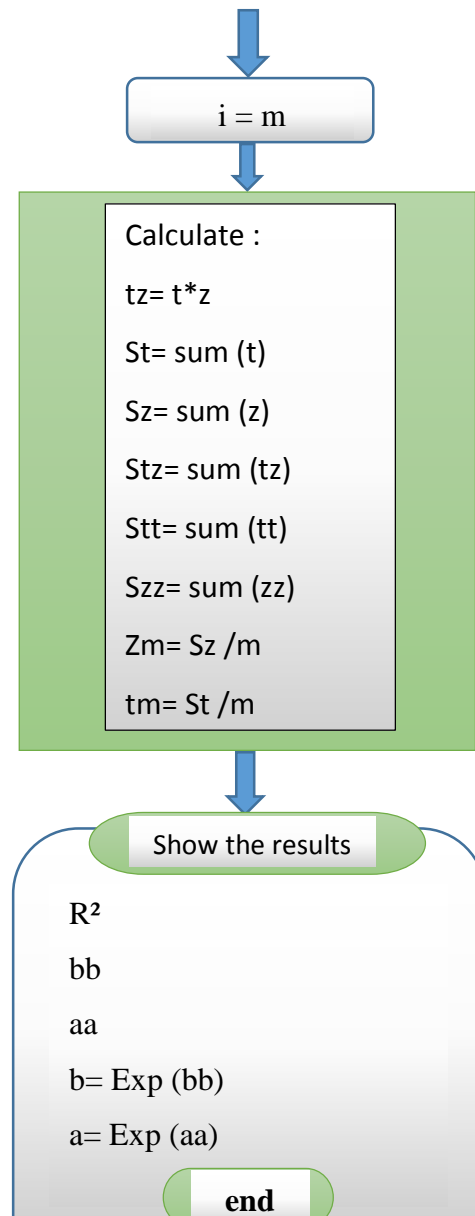
III.4.6.2. Example of Matlab:

```

1  clear
2  clear all
3  y=input('y=');
4  mm=size(y);
5  m=mm(1,2);
6  dt=input('dt=');
7  for i=1:m;
8      t(i)=(i-1)*dt;
9      z(i)=log(y(i));
10     tt(i)=(t(i)).^2;
11     zz(i)=(z(i)).^2;
12 end
13 tz=t.*z;
14 st=sum(t);
15 sz=sum(z);
16 stz=sum(tz);
17 stt=sum(tt);
18 szz=sum(zz);
19 zm=sz/m;
20 tm=st/m;
21 R=(m*stz-st*sz)/(sqrt(m*stt-st^2)*sqrt(m*szz-sz^2));
22 bb=(m*stz-st*sz)/(m*stt-st^2);
23 aa=zm-bb*tm;
24 'constant a'
25 a=exp(aa)
26 'constant b'
27 b=exp(bb)
28 'constant RR'
29 RR=R*R
30
31
32

```

Fig (III-17): Calculation of a, b, R² by using Matlab program.



Tables (III-2), (III-3) and (III-4) shown below, present the Statistical parameters obtained from selected thin layer drying models (Newton, Henderson and Pabis, Logarithmic) and the extracted model for solar cabinet drying of potato, carrot and apple slices.

The model suitability was determined by considering the highest value of coefficient of determination (R^2), and least value of chi square (χ^2) and root mean square error (RMSE). From tables (III-2), (III-3) and (III-4) it can be observed that the logarithmic model has the highest value of coefficient of determination (R^2), and corresponding least value of chi square (χ^2) and root mean square error (RMSE) among the three models used. So it has been concluded that the logarithmic model is best suited for describing the drying behaviour of the thin layer of potato, carrot and apple samples.

Models		R ²	RMSE	SSE	χ^2	a	b	g	k
Newton	1	0.9437	0.11472	0.0123	0.0132				0.00701
	2	0.9175	0.09799	0.00896	0.0096				0.00418
	3	0.9236	0.11132	0.01144	0.01239				0.00414
Henderson and Pabis	1	0.9317	0.102367	0.00978	0.01048				0.00790
	2	0.898	0.08447	0.00666	0.0071				0.00486
	3	0.9106	0.100159	0.00926	0.01003				0.00470
Logarithmic	1	0.9565	0.074230	0.00514	0.00551	1.3696	-0.2631		0.00493
	2	0.9839	0.033796	0.00107	0.00114	88.93	-87.87		0.000031
	3	0.9828	0.042902	0.00169	0.00184	75.62	-74.58		0.000037
Model	1	0.915	0.108068	0.01090	0.01168	1.1553	0.992		
	2	0.880	0.122645	0.01404	0.01504	1.1561	0.995		
	3	0.897	0.102915	0.00977	0.01059	1.1122	0.995		

Table (III-2): Thin layer drying models for describing drying of potato slices.

Models		R ²	RMSE	SSE	χ^2	a	b	g	k
Newton	1	0,9483	0,14609	0,01956	0,02134				7,53E-03
	2	0,9557	0,09713	0,00865	0,00944				6,95E-03
	3	0,9618	0,08552	0,00670	0,00731				6,07E-03
Henderson and Pabis	1	0,9359	0,103829	0,00988	0,01078	1,132			8,39E-03
	2	0,9461	0,08925	0,00730	0,00797	1,095			7,57E-03
	3	0,9532	0,07781	0,00555	0,00605	1,086			6,60E-03
Logarithmic	1	0,9732	0,062659	0,00359	0,00393	1,581	-0,5097		3,99E-03
	2	0,9882	0,03912	0,00140	0,00153	1,778	-0,7526		2,89E-03
	3	0,9969	0,01880	0,00032	0,00035	2,2994	-1,289		1,82E-03
Model		0,9191	0,103843	0,00988	0,01078	1,1322	0,9916		
		0,9323	0,089217	0,00729	0,00796	1,095	0,9925		
		0,9427	0,078615	0,00566	0,00618	1,10858	0,9934		

Table (III-3): Thin layer drying models for describing drying of carrot slices.

Models		R ²	RMSE	SSE	χ^2	a	b	g	k
Newton	1	0,9365	0,116029	0,01234	0,01346				4,92E-03
	2	0,9516	0,099762	0,00912	0,00995				5,89E-03
	3	0,9623	0,092078	0,00783	0,00848				5,69E-03
Henderson and Pabis	1	0,9214	0,10141	0,00943	0,01028	1,13			5,63E-03
	2	0,9406	0,08976	0,00739	0,00806	1,1044			6,52E-03
	3	0,9518	0,08094	0,00605	0,00655	1,108			6,30E-03
Logarithmic	1	0,991	0,03295	0,00099	0,00109	3,83	-2,7655		9,75E-04
	2	0,993	0,02999	0,00082	0,00089	2,97	-1,94		1,35E-03
	3	0,9933	0,028498	0,00075	0,00081	2,03448	-0,999		2,08E-03
Model	1	0,9214	0,101407	0,00943	0,01028	1,130269	0,99438		
	2	0,9407	0,089767	0,00739	0,00806	1,104409	0,9935026		
	3	0,9519	0,080942	0,00605	0,00655	1,108333	0,993717		

Table (III-4): Thin layer drying models for describing drying of apple slices.

III.5. Conclusion:

This chapter was based on describing of the experimental steps that were accomplished during the period between February and May 2019. Depending on the necessary materials and special measuring instruments, the experiments were carried out in good conditions, and that was a main reason for the recorded positive results after drying of samples of potato, carrot and apple in different thicknesses. Also using some of mathematical models as the logarithmic model to describe the drying behaviour of potato slices, which was very consistent with our experimental results and has been the best among all the models.

«References»

- [1]: Hanafi, A., and D. Alkama. "Stratégie d'amélioration du confort thermique d'une place publique d'une ville saharienne'Biskra/Algérie'." *Revue des Energies Renouvelables* 19.3 (2016): 465-480.
- [2]: Ayensu, A. Dehydration of food crops using a solar dryer with convective heat flow. *Solar Energy*, 59(1997) 121-126
- [3]: Rahman, M. S., C. O. Perera, and C. Thebaud. Desorption isotherm and heat pump drying kinetics of peas. *Food Research International*, 30(1998) 485–491.
- [4]: Lahsasni, S., M. Kouhila, M. Mahrouz, and J. T. Jaouhari. Drying kinetics of prickly pear fruit (*Opuntia ficus indica*). *Journal of Food Engineering*, 61(2004) 173–179.
- [5]: V. Shanmugam, E. Natarajan, (2006) Experimental investigation of forced convection and desiccant integrated solar dryer *Renewable Energy* 31, 1239–1251
- [6]: Hossain, M.A. and B.K. Bala. 2002. Thin layer-drying characteristics for green chilli. *Drying Technology*, 20(2): 489–505.
- [7]: Crank J (1975) *The mathematics of diffusion*. Clarendon, Oxford, England.
- [8]: H. Togrul, Suitable drying model for infrared drying of carrot, *Journal of Food Engineering*, 77 (2006) 610–619.
- [9]: Babalis, S. J., & Belessiotis, V. G. Influence of drying conditions on the drying constants and moisture diffusivity during the thin-layer drying of figs. *Journal of Food Engineering*, 65(2004) 449–458.
- [10]: <https://www.investopedia.com/corporate-finance-and-accounting-4689821> consulted in 11/06/2019

Chapter IV

Results

and

discussion

IV.1. Introduction:

The solar drying is simply the process of moisture removal from a wet product by using of a special equipments and different techniques. This process is influenced by a several factors as the solar radiation, temperature and the relative humidity, which are considered as main reasons for the drying success with good results. The obtained results are extracted experimentally and then it is being discussed and interpreted.

So in this chapter, we are going to present a set of figures related to the curves that translate the results, which were obtained experimentally during the drying process and then explaining and interpreting this curves that describe the main factors which were influencing on the drying operation.

IV.2. Variation in solar radiation intensity:

Figures (IV-2a), (IV-2b) and (IV-2c) present the curves of solar radiation intensity variation versus time during the day, for drying experiments of three different products (potato, carrot and apple), each product was carried out on three days by using a solar air collector inclined by 38° . The main purpose of this solar radiation is to heat the absorber plate and for that, the passed air will be heated by convection to use it in the drying operation. The solar radiation increased by time and reached the max level at around 13pm and then it decreased another time, and we have observed the following results:

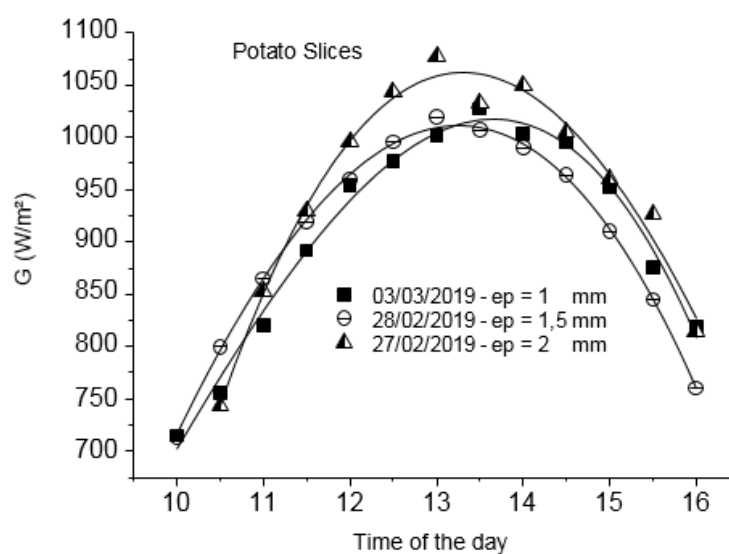


Fig (IV-2a): Variation of solar radiation intensity in 1-3 days of potato drying.

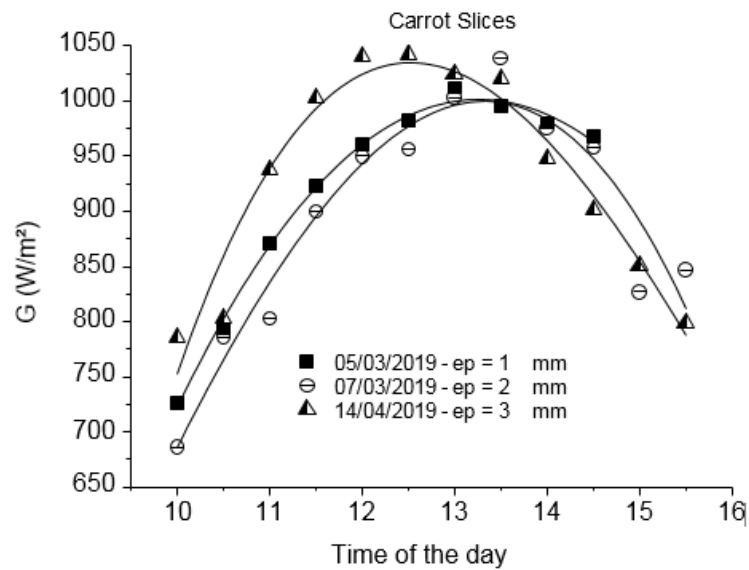


Fig (IV-2b): Variation of solar radiation intensity in 1-3 days of carrot drying.

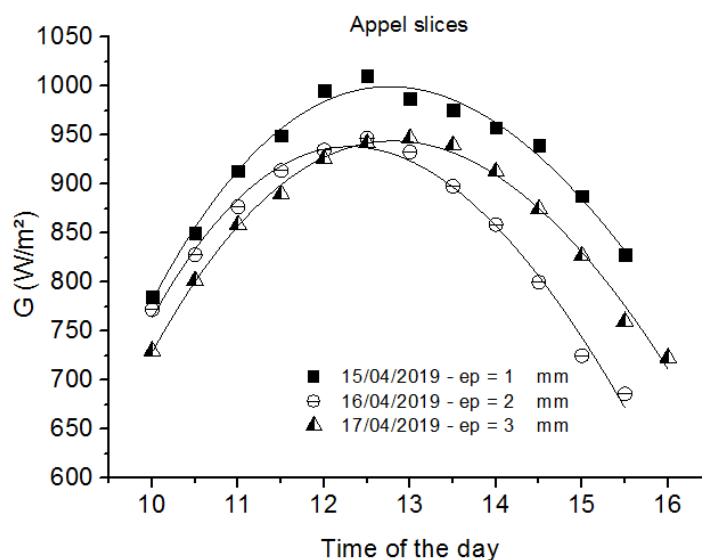


Fig (IV-2c): Variation of solar radiation intensity in 1-3 days of apple drying.

For potato experiments: the solar radiation intensity surpassed 1000 w/m^2 in all the three days, but the maximum recorded value was 1077 w/m^2 in 27 February 2019 at 12:30 pm, see Fig (IV-2a). For carrot experiments: the maximum radiation intensity was 1042 W/m^2 in 14 April 2019 at 13:30 pm and it record values over 1000 w/m^2 for a longer period between 12 and 14 pm, also the all three days was surpassed this value, see Fig (IV-2b).

As for apple experiments: we observed lower values compared to the other days, where the maximum radiation intensity value was 1011 w/m^2 in 15 April 2019 at 12:30 pm and it

surpassed 1000 w/m^2 just in this day, where the rest two days recorded a value of 947 w/m^2 as a maximum value, see Fig (IV-2c).

IV.3. Variation of the average temperature of the absorber plate:

Figures (IV-3a), (IV-3b) and (IV-3c) explain the variation of average temperature of the absorber plate for the solar collector with time, during 9 days of drying experiments. This absorber plate is the main reason for heating the air passed through the drying room due to its high temperature obtained from the solar radiation, which is distributed at this absorber. These curves have the same form with the solar radiation curves because it increase to reach a maximum level then it decrease by time of the sunset, and we have recorded the following results:

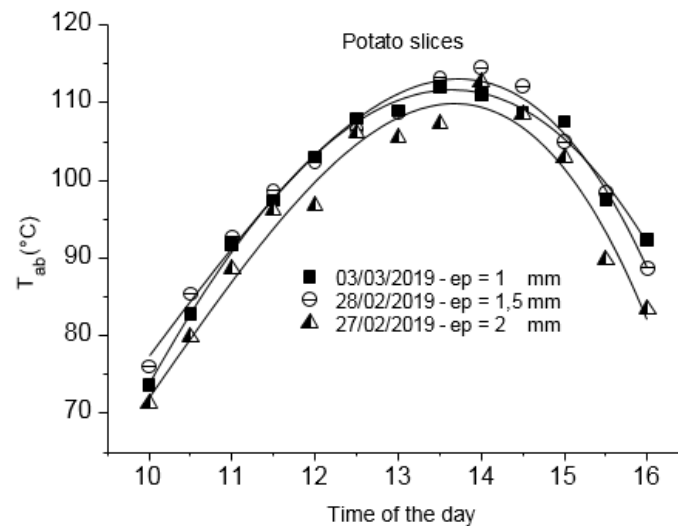


Fig (IV-3a): Average absorbing surface temperature versus time for three days of potato drying.

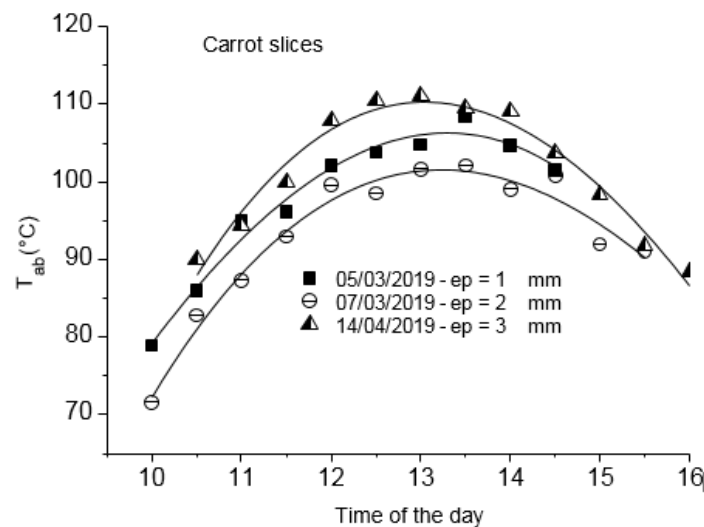


Fig (IV-3b): Average absorbing surface temperature versus time for three days of carrot drying.

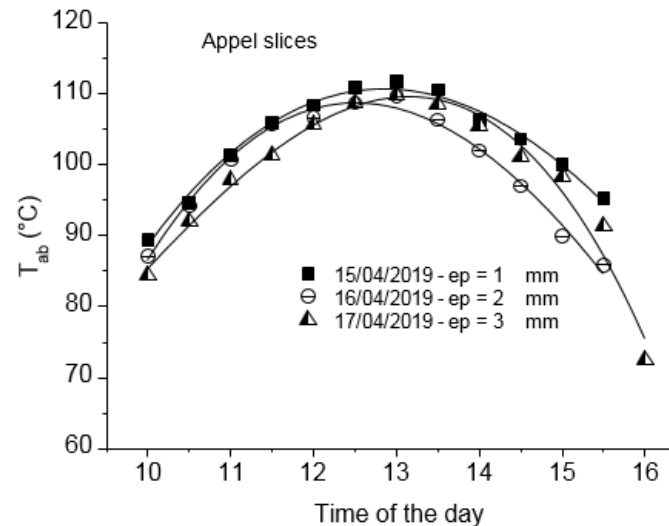


Fig (IV-3c): Average absorbing surface temperature versus time for three days of apple drying.

For potato experiments: the highest recorded average temperature of this absorber was $114\text{ }^{\circ}\text{C}$ in 28 February 2019, which corresponds to a value of 990 W/m^2 of solar radiation at 14 pm, while in other days the temperature have exceeded a value of $110\text{ }^{\circ}\text{C}$, see fig (IV-3a).

For carrot experiments: it was observed that all the days have a maximum values between 100 to $112\text{ }^{\circ}\text{C}$ of average absorbing temperature, while the best recorded value was $111\text{ }^{\circ}\text{C}$ in 14 April 2019, which corresponds 1042 w/m^2 of solar radiation intensity at 13 pm, see fig (IV-3b).

For apple experiments: a maximum value of average temperature absorbing equal $112\text{ }^{\circ}\text{C}$ was observed in 15 April 2019 at 13 pm and which corresponds 988 w/m^2 of solar radiation intensity, however in the rest days it has not exceeded of $110\text{ }^{\circ}\text{C}$ because the solar radiation values were lower than the other experiments, see Fig (IV-3c).

IV.4. variation of drying room inlet temperature:

Figures (IV-4a), (IV-4b) and (IV-4c) present the variation of drying room inlet temperature versus time curves, for different experiments of the thin layer drying of potato, carrot and apple. So when the heated air comes out of the solar air collector, it moves through a special channel and then its temperature is measured directly at the drying room inlet, and we have observed the following results:

It was observed that the temperature curves are increasing gradually to reach a maximum value and decreasing in the end due to the falling in values of solar radiation intensity.

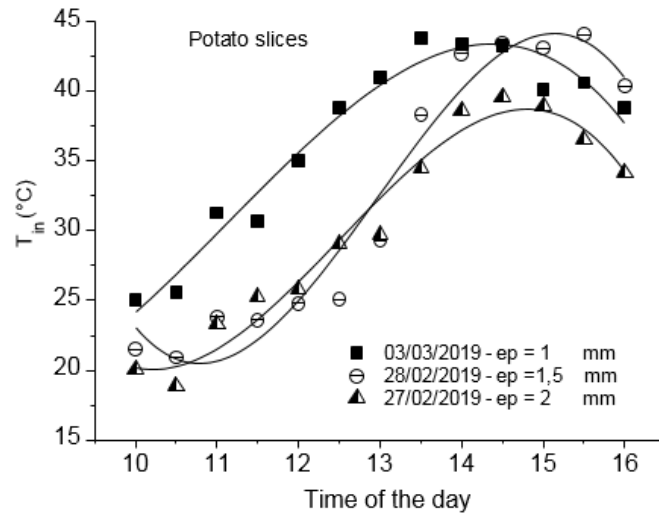


Fig (IV-4a): Variation of the drying room inlet temperature with time for 3 days of potato drying.

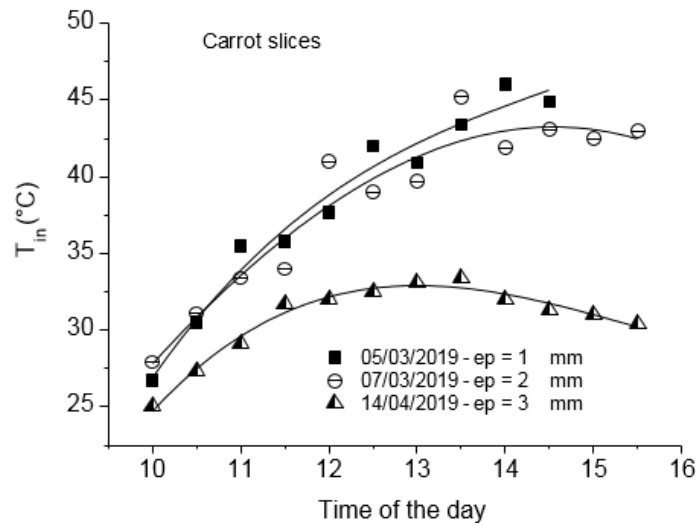


Fig (IV-4b): Variation of the drying room inlet temperature with time for 3 days of carrot drying.

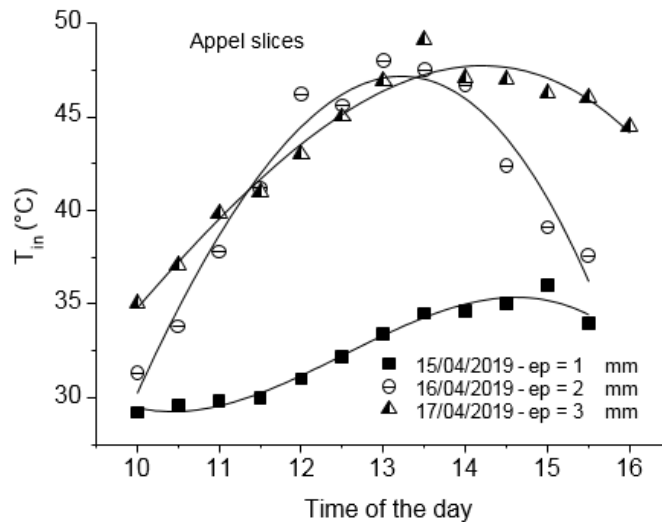


Fig (IV-4c): Variation of the drying room inlet temperature with time for 3 days of apple drying.

For potato tries, it was noted that the third try was the best one because of the highest recorded values of temperature, and the difference in temperature between the first and the other tries which was high until 14:00 and at this time there was an agreement in temperature with the second try and then, the second one become higher until the end. The highest value of temperature was 43.8 °C for the first try and 43.5 °C for the second try see fig (IV-4a).

For carrot tries, see fig (IV-4b) the curve behaviour of the first try was very close to the second one, which they intersect in five points, and the maximum value of drying room inlet temperature was 46 °C for the first try and 45.2 °C for the second. While the variation in temperature was lower in the third try, which it did not surpassed a value of 34 °C because of the air velocity.

As for apple tries, the second and the third tries were in good agreement in temperature between 12:00 and 14:30 pm, but the third one was the best in the rest of time and its maximum temperature was 49 °C. While the change in temperature in the third try was low, although the solar radiation was the highest and the reason for that was the air velocity, which was influencing on the air circulation inside of the solar collector, see fig (IV-4c).

IV.5. Variation of drying room temperature:

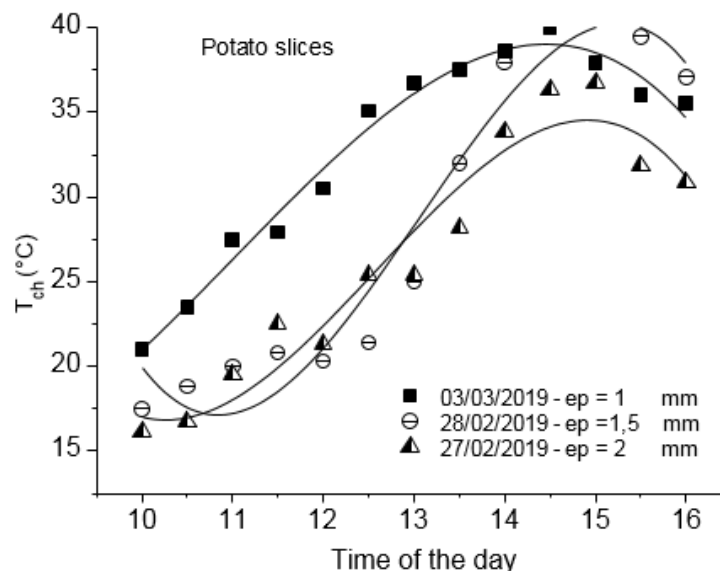


Fig (IV-5a): Variation of drying room temperature versus time for potato slices.

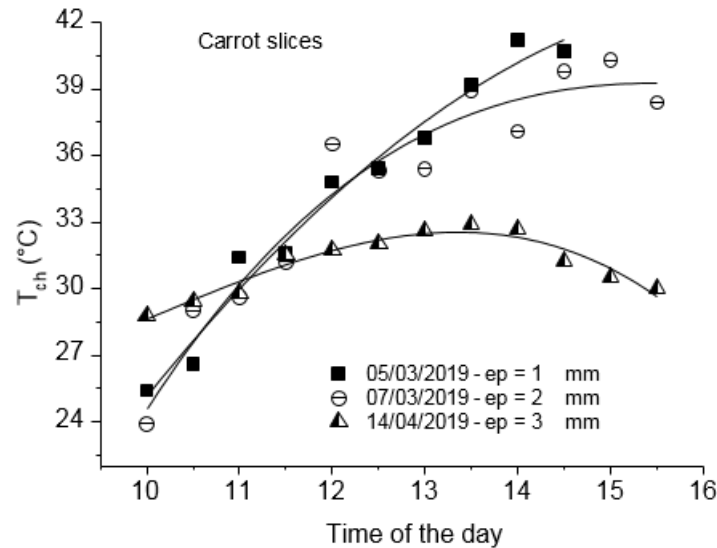


Fig (IV-5b): Variation of drying room temperature versus time for carrot slices.

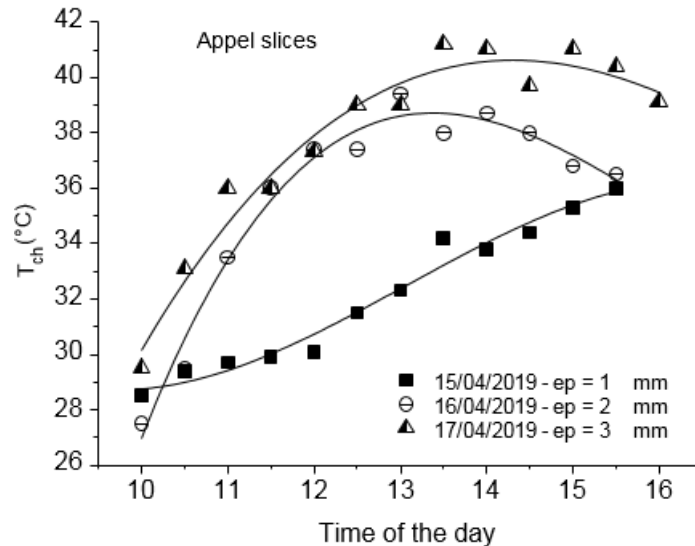


Fig (IV-5c): Variation of drying room temperature versus time for apple slices.

Figures (IV-5a), (IV-5b) and (IV-5c) show the change in temperature inside the drying room with time for three products to be dried with different thicknesses, and we observed the following results:

For potato samples, the temperature of the drying room is increasing significantly over time in all cases but it is starting of falling in the end of the drying, and the best recorded value was 40 °C, see fig (IV-5a).

As for carrot samples, see fig (IV-5b) the temperature changes upward over time and there was a match between the first and the second case in the temperature. However, the change was lower in the last case with thickness of 3mm, and this is due to the drying room inlet temperature, which was lower too.

Concerning of apple samples, the increase in drying room temperature is always existing and logically in all cases, the last experiment with 3mm of thickness was the best in temperature most of time, which it recorded a maximum value of 41 °C, while the first one was less in temperature due to the drying room inlet temperature, see fig (IV-5c).

IV.6. Variation of product temperature:

The variation of product temperature with time for drying potato, carrot and apple with different thicknesses is shown in figures (IV-6a), (IV-6b) and (IV-6c) and we have noted the following results:

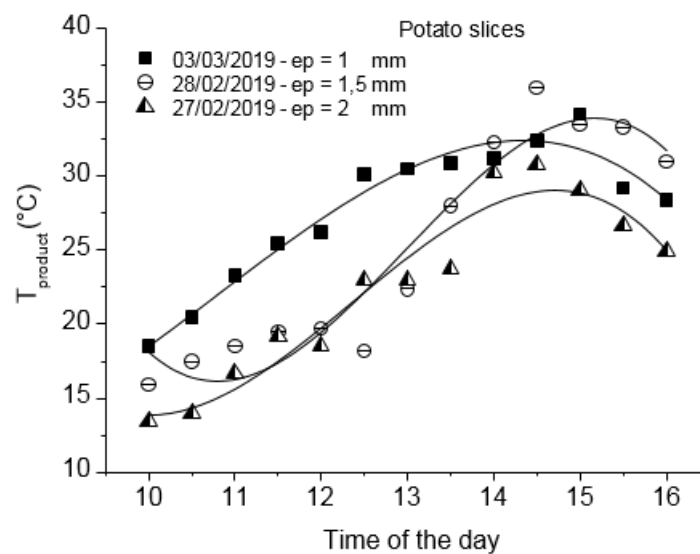


Fig (IV-6a): Variation of product temperature versus time for different thicknesses of potato slices.

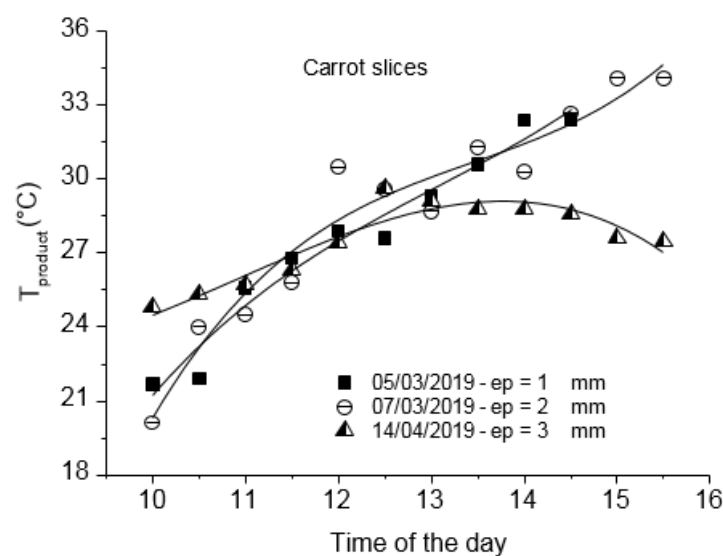


Fig (IV-6b): Variation of product temperature versus time for different thicknesses of carrot slices.

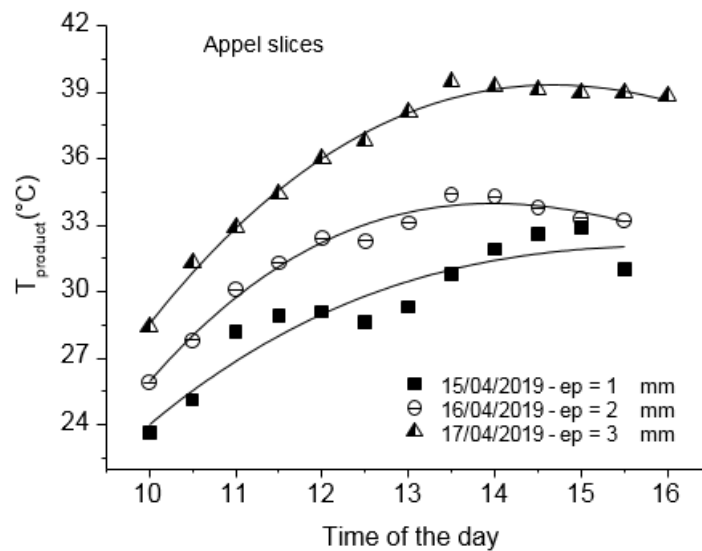


Fig (IV-6c): Variation of product temperature versus time for different thicknesses of apple slices.

Potato drying curves shows that the experiment, which was dealing with 1 mm of thickness, has the best variation in product temperature in most of time, although the slices with 1.5 mm has the highest variation in the end between 14:30 and 16:00 pm with a maximum value recorded of 36 °C. While the slices with 2 mm has an agreement in temperature with 1.5 mm of thickness just in the beginning of the drying, see fig (IV-6a).

For carrot drying curves, see fig (IV-6b), it was noted that there was a good variation in temperature product for carrot with 1 and 2mm in most of time, and their maximum temperature equal 32.4 and 34.1 °C respectively. but the slices with 3mm of thickness, has a good variation just in the beginning and then, it was decreased because the temperature in drying room was lower than the other tries, see fig (IV-5b)

With regard to the curves of apple drying, the experiment that was dealing with 3mm of thickness has the best variation in temperature product in all time and with high difference between it and the other tries, and it reached to high value of 39.5 °C, see fig (IV-6c).

IV.7. The change in relative humidity of products:

Figures (IV-7a), (IV-7b) and (IV-7c) that shown below present the variation in relative humidity for each product with different sizes inside the drying room and during the drying periode. It was observed that all curves are decreasing over time from the maximum to reach a minimum value of relative humidity, and that explain the high moisture content of the wet product in the process beginning, which was gradually losing its moisture until to be dried.

We also note that these curves take an opposite shape to those related with product temperature, see fig (IV-6a), (IV-6b) and (IV-6c) that it is increasing as we said previously, this confirms that the increase in temperature is always accompanied by decreasing in humidity.

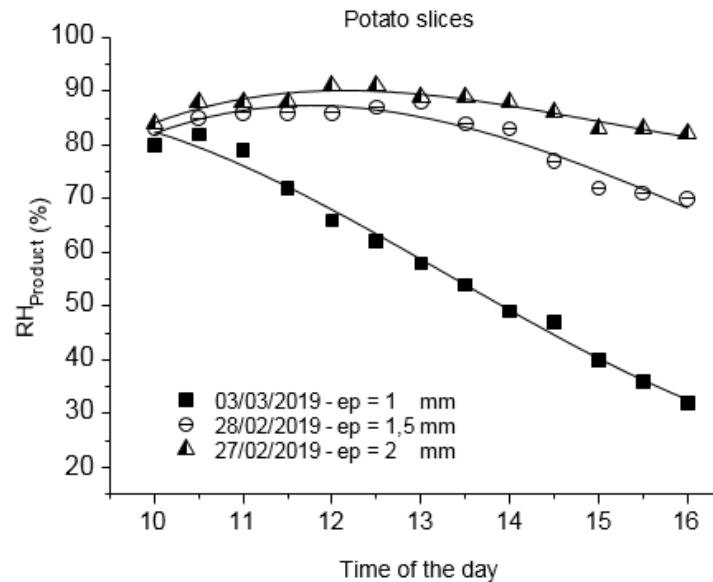


Fig (IV-7a): The change in relative humidity of product versus time for potato drying.

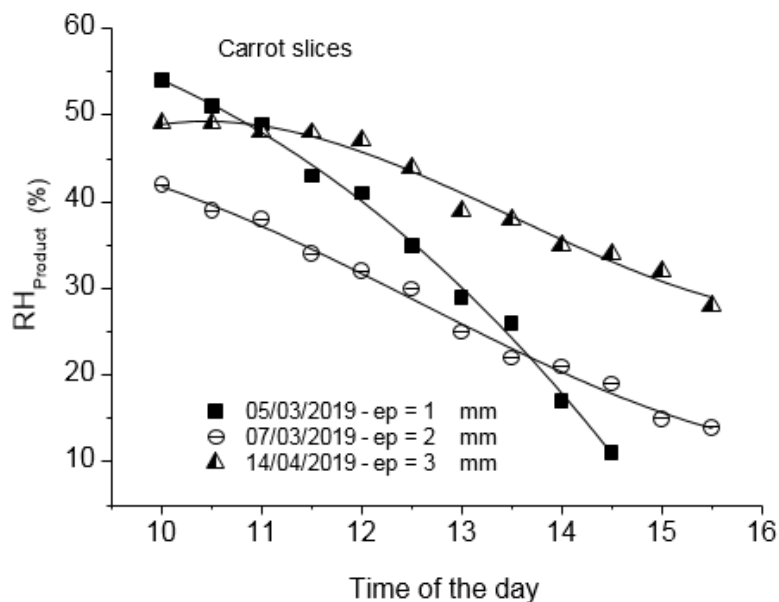


Fig (IV-7b): The change in relative humidity of product versus time for carrot drying.

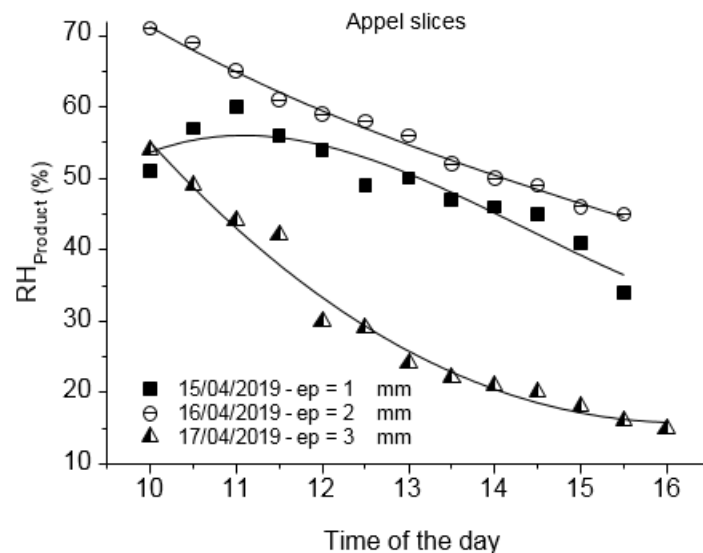


Fig (IV-7c): The change in relative humidity of product versus time for apple drying.

IV.8. The change in liquid mass loss during time of each product:

Figures (IV-8a), (IV-8b) and (IV-8c) below, shows the curves of variation in liquid mass loss from the wet product during the drying time until the end, each product loses its water by evaporation due to the heated air, which is circulate in the drying room. These curves increase over time and that means the increase in the missing liquid mass each time, and then it stop and this indicates the end of the drying process, and we have observed the following results:

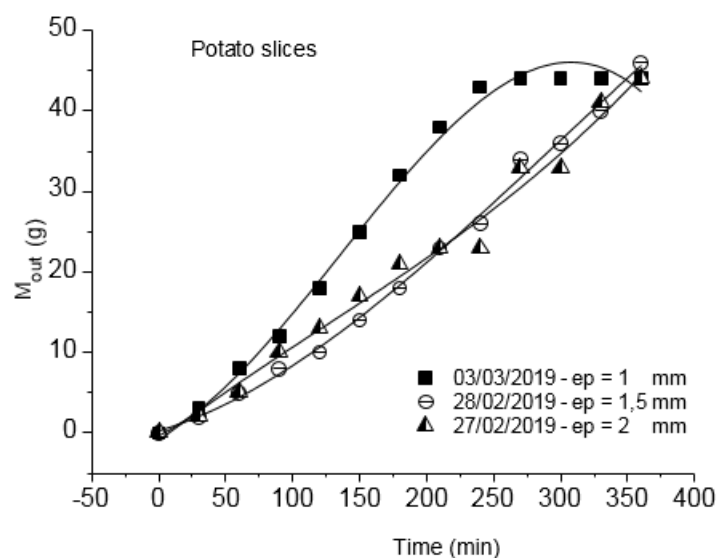


Fig (IV-8a): Variation in liquid mass loss during time for potato drying.

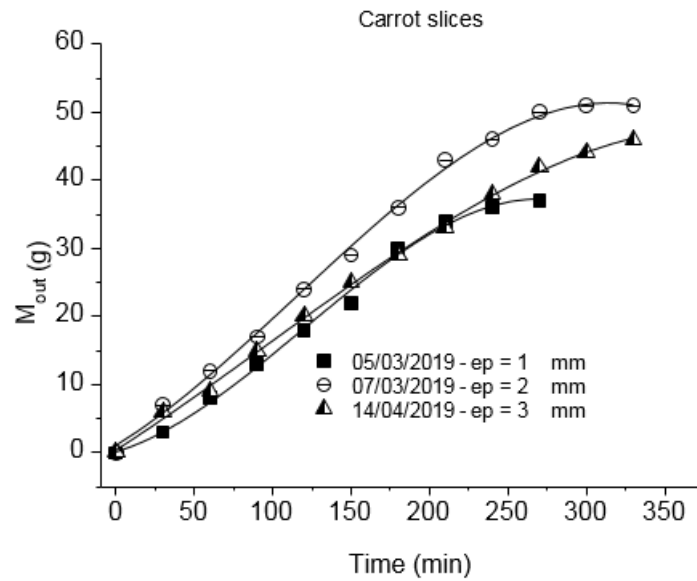


Fig (IV-8b): Variation in liquid mass loss during time for carrot drying.

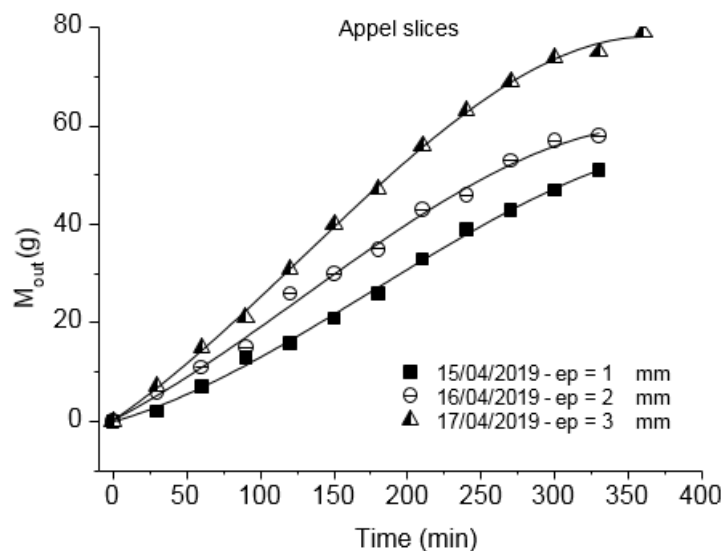


Fig (IV-8c): Variation in liquid mass loss during time for apple drying.

For potato samples, the experiment with 1 mm was the best in most of time in mass losing, while the other experiments were in good agreement and all that due to the drying room temperature and difference in the thickness, and the highest recorded value was 46 g of liquid mass loss from the total mass of 60 g.

As for carrot samples, all the experiments had an agreement in liquid mass loss with slight superiority to the experiment that is related to 2 mm of thickness and it recorded a maximum value of 51 g of liquid mass loss from the total mass of 60 g.

The experiments, which were dealing with apple samples were the best at all in losing of the liquid mass, it recorded a value of 79 g as a maximum of mass loss from the total mass of 100 g, and it has been observed that the increase in thickness is accompanied by an increase in loss of liquid mass.

IV.9. Determination of reduced moisture ratio MR:

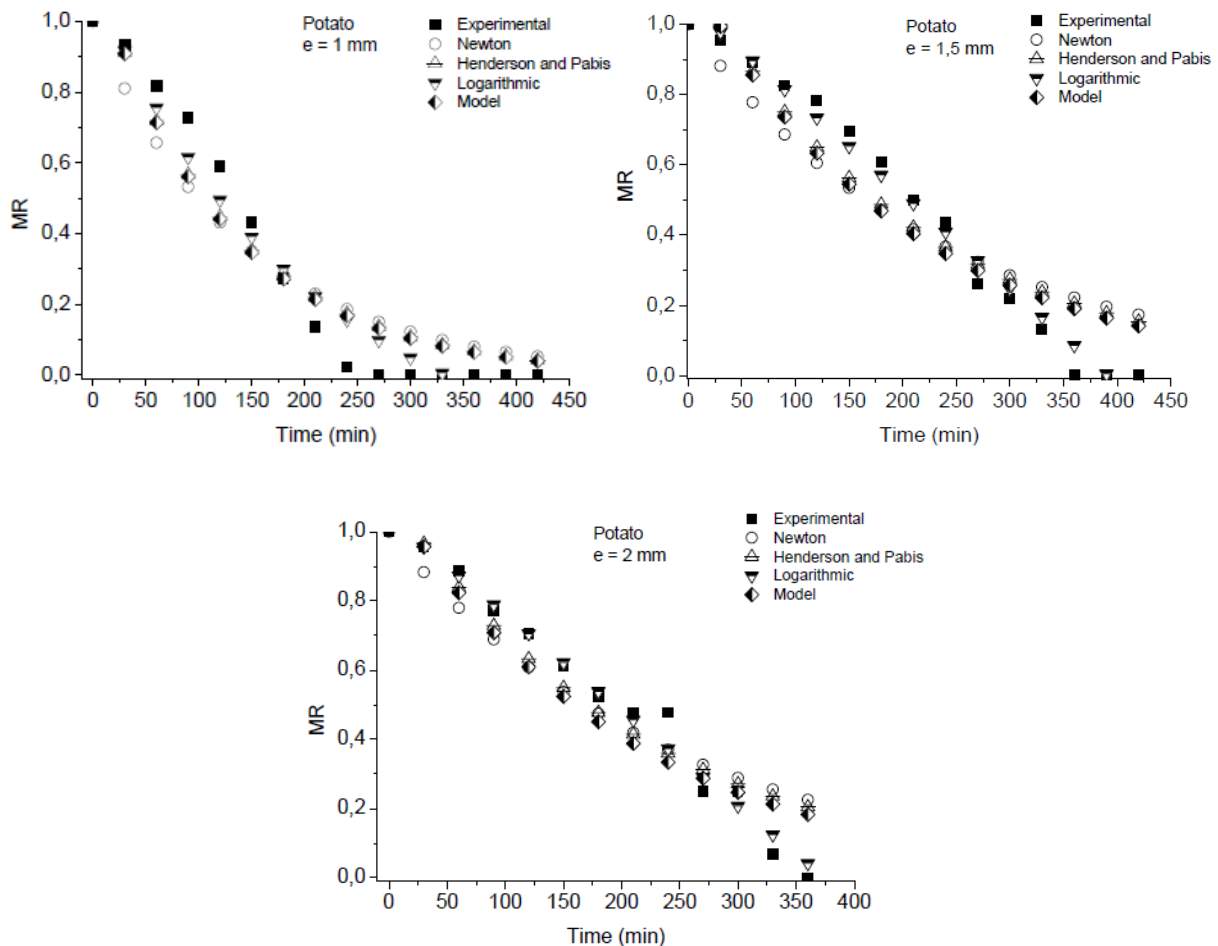


Fig (IV-9a): The moisture ratio versus drying time for different models of potato slices with 1, 1.5, and 2 mm of thickness.

We have presented in figure (IV-9a) the curves of reduced moisture ratio MR as a function of time, determined by the extracted model, newton and the logarithmic model in addition to Henderson and Pabis model and those obtained experimentally, each figure represents a different thickness of potato; 1, 1.5 and 2mm respectively. It was observed in figure (IV-9a) that the experimental results were close in most of drying time to the logarithmic and the extracted model. However, the logarithmic model was in good agreement with the

experimental results, and that confirms that the logarithmic model could be the best to describe the drying behaviour of potato slices.

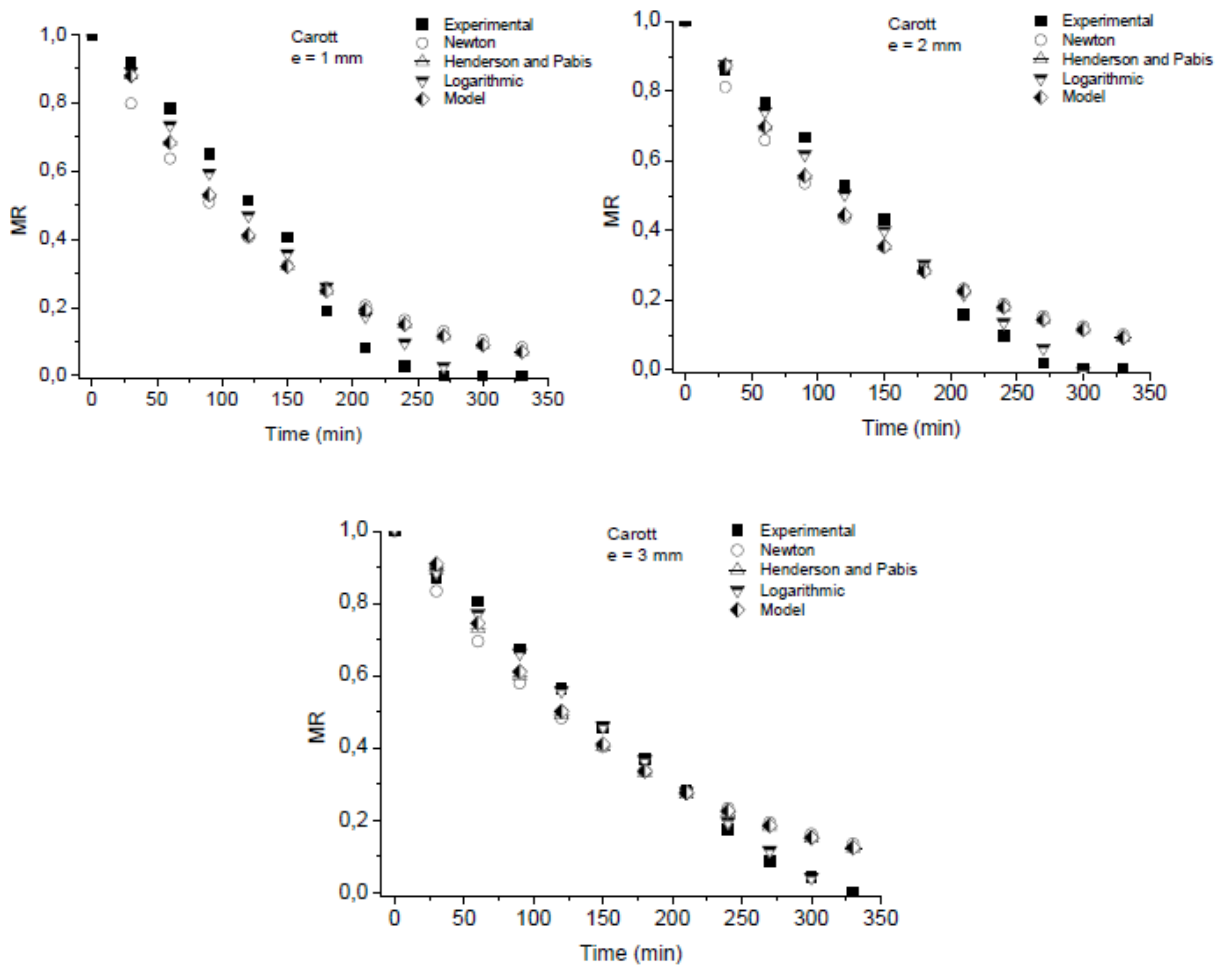


Fig (IV-9b): The moisture ratio versus drying time for different models of carrot slices with 1, 2 and 3mm of thickness.

Figure (IV-9b), presents the variations of experimental and predicted moisture ratio values with drying time, which show the moisture ratio values predicted by a several models as Newton and the Logarithmic model, in addition to Pabis and Henderson model. These models compared with the experimental results and our extracted model for solar drying of carrot slices with 1, 2 and 3mm of thickness respectively. It can be observed in all curves with different in thickness that the logarithmic model was more agreement with the experimental results, while the extracted model was closer than the rest of the other models, but it was in agreement to them in the end of drying. So we can say that the logarithmic model is suitable for explain the drying behaviour of carrot.

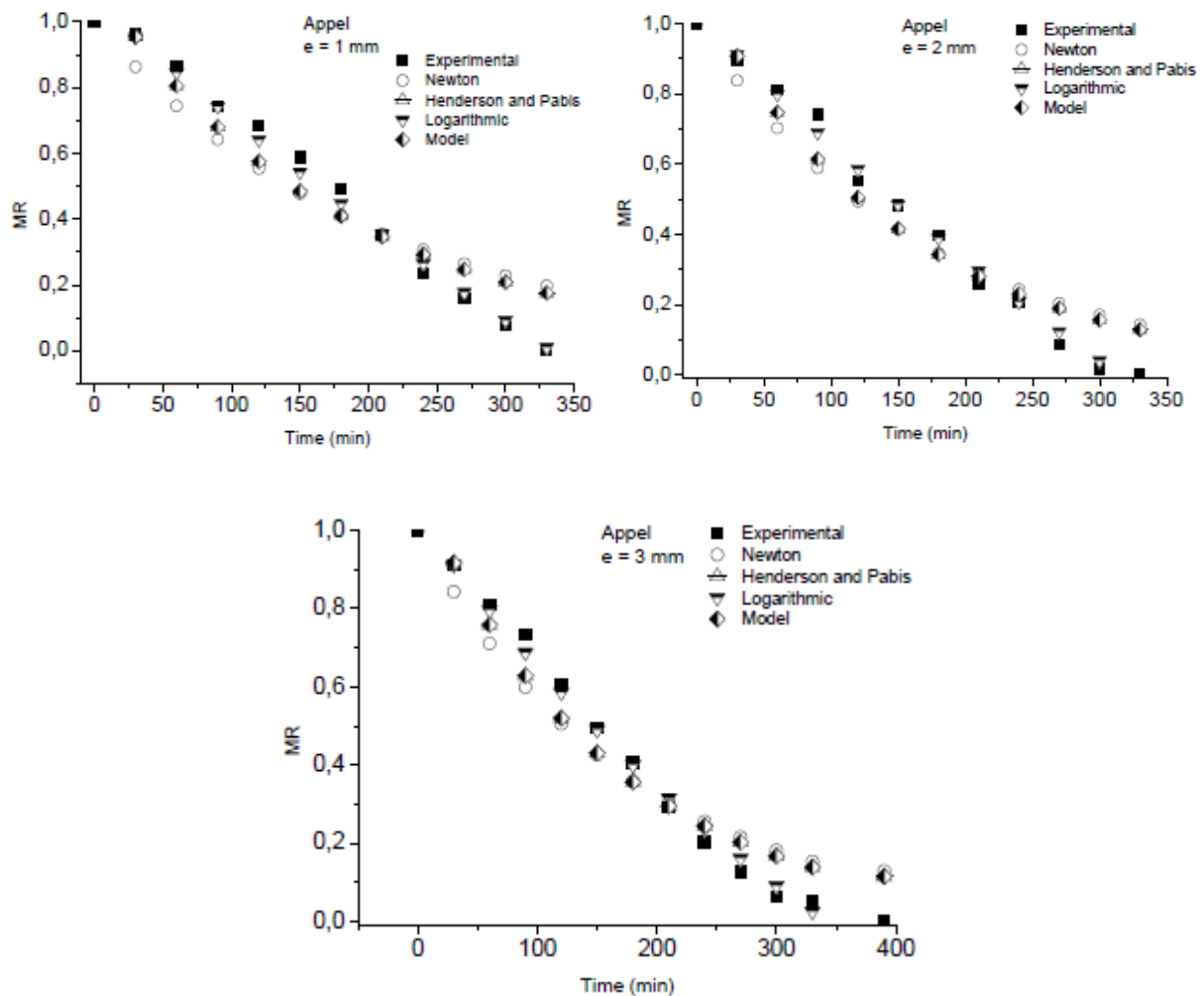


Fig (IV-9c): The moisture ratio versus drying time for different models of apple slices with 1, 2 and 3mm of thickness.

We have presented in figure (IV-9c), the curves of reduced moisture ratio MR, determined by a several models (newton, logarithmic, Henderson and Pabis) compared to our extracted model with the experimental results as function of time, each picture represents a different thickness of apple; 1, 2 and 3mm respectively. It was observed that the logarithmic model was in good agreement with the experimental results and better than all the other models in the all different curves, while the extracted model was in agreement to Henderson and Pabis and newton models in most of time. This allowed us to conclude that we could chose the logarithmic model as a suitable model for explain the drying behaviour of apple slices.

IV.10 . Conclusion:

In this fourth and last chapter, we have seen a set of curves that reflect the most important factors affecting the process of solar drying, which gradually change over time. The main purpose of this chapter was to investigate the various changes that occur on the basic factors from the beginning to the end of the drying process and to provide the appropriate explanations. It has been observed that, these factors affect each other such as solar radiation that directly affect the average temperature of the absorber plate, where the highest value of solar radiation intensity was 1042 W/m^2 which corresponds to 111°C as the value of the absorber plate. As for the temperature degrees of the heated air in the inlet of the drying room was the first reason, which was influencing on the temperature of the drying room, dried product and its relative humidity. From another side we found that the logarithmic model, which is determined the reduced moisture ratio was the best for describing the drying behaviour of the used products.

*General
conclusion*

«General conclusion»

In conclusion, this experimental study mainly has been carried out to investigate the solar drying behaviour of different agricultural products under natural convection, by using an indirect solar dryer, which was designed and constructed previously with local materials. This study considers the thin layer drying under various conditions, for three different thicknesses and quantities of potato, carrot and apple with round slices form.

The experimental data were fitted to different mathematical moisture ratio models to compare them with the extracted model.

Repetitive tests show that the drying speed are strongly influenced by the shape and the size of samples for each product and that confirms the choice of small thicknesses is always accompanied with drying time faster, as we noted that the carrot samples were faster in drying because it basically has a least moisture than potato and apple.

From another side in thicker slices (3 mm), the hot air hardly passes through the samples and decreases the moisture gradient and moisture diffusivity especially that we are dealing with natural convection to pass the heated air through the drying room.

Moreover, the effect of the solar radiation intensity is the primary factor to accomplish the drying process as purpose of heating the absorbing plate; the tests recorded good results of solar radiation and average temperature absorbing with maximum values of 1077 W/m^2 and $114 \text{ }^\circ\text{C}$ respectively.

As for the product temperature, it is influenced directly by the temperature in the inlet and the inside of the drying room, which works on removing the moisture by evaporation, and that explain accompany of temperature increasing with decreasing in relative humidity.

In addition, the relative humidity of product to be dried is high at the beginning of experiments due to the high moisture content of dried product samples, then decrease gradually with the time until the end of test.

Finally, a several mathematical models were used to determine the reducing moisture ratio, and the logarithmic model, showed the best fit to the experimental data with the highest average values of R^2 and the lowest average values of χ^2 and $RMSE$. While our extracted model was in agreement with the other models as Newton, Pabis and Henderson, and it was better just in some times.

Finally, I would like to say that although the difficult of the solar drying under the natural convection, which is need for very long time, in addition to the solar dryer, which was designed for the forced convection and it was not without heat losing, we were able to accomplish the tests in a good way. Also, we have extracted satisfactory results that no one was expected it. So we hope to achieve other methods of solar drying and include it within the graduation projects in the future because the solar energy in our region is a treasure and it is wonderful to exploit it for the sake of science.

Abstract :

Our experimental study was aimed to investigate the solar drying behaviour of three different food products under natural convection by using an indirect solar dryer, which was designed and constructed previously with local materials. This study focuses on thin layer drying of potato, carrot and apple, which were cutted into circular slices with three different thicknesses. We have extracted a mathematical moisture ratio model based on the obtained experimental data to compare it with the other used models as the logarithmic model, Newton model and Pabis and Henderson model. The results show that, the drying kinetics depend, on the thickness and the size of samples in addition, that the logarithmic model was selected as the best model to describe this drying behaviour.

Keywords: solar drying, natural convection, thin layer drying, potato, carrot, apple.

ملخص:

كانت دراستنا التجريبية تهدف إلى دراسة سلوك التجفيف الشمسي لثلاثة منتجات غذائية مختلفة تحت تأثير الحمل الحراري باستخدام مجفف شمسي غير مباشر، تم تصميمه وصنعه مسبقاً باستخدام مواد محلية. تركز هذه الدراسة على تجفيف الطبقة الرقيقة من البطاطا والجزر والتفاح، والتي تم تقطيعها إلى شرائح دائرية بثلاثة سماكات مختلفة. لقد استخرجنا نموذجاً رياضياً لنسبة الرطوبة استناداً إلى البيانات التجريبية التي تم الحصول عليها لمقارنته مع النماذج المستخدمة الأخرى مثل النموذج اللوغاريتمي ونموذج نيوتن ونموذج بابيس وهيندرسون. أظهرت النتائج أن حركات التجفيف تعتمد على سمك وحجم العينات بالإضافة إلى اختيار النموذج اللوغاريتمي كأفضل نموذج لوصف سلوك هذا التجفيف.

الكلمات المفتاحية: التجفيف الشمسي، الحمل الحراري الحر، تجفيف الطبقة الرقيقة، البطاطس، الجزر، التفاح.

Résumé :

Notre étude expérimentale visait à étudier le comportement au séchage solaire de trois produits alimentaires différents en convection naturelle en utilisant un séchoir solaire indirect, conçu et construit auparavant avec des matériaux locaux. Cette étude porte sur le séchage en couche mince de pommes de terre, de carottes et de pommes, qui ont été découpées en tranches circulaires de trois épaisseurs différentes. Nous avons extrait un modèle mathématique du taux d'humidité basé sur les données expérimentales obtenues pour le comparer aux autres modèles utilisés tels que le modèle logarithmique, le modèle de Newton et le modèle de Pabis et Henderson. Les résultats montrent que la cinétique de séchage dépend en plus de l'épaisseur et de la taille des échantillons, et que le modèle logarithmique a été sélectionné comme meilleur modèle pour décrire ce comportement de séchage.

Mots clés : séchage solaire, convection naturelle, séchage en couche mince, pomme de terre, carotte, pomme.